Universidade de Aveiro Secção Autónoma de Ciências da Saúde
2012

Roberto Alexandre dos Santos Dias

Fosforilação da PPA na colocalização da PPA/$G_{\alpha o}$ e ativação da STAT3

APP phosphorylation on APP/$G_{\alpha o}$ colocalization and STAT3 activation

Universidade de Aveiro Secção Autónoma de Ciências da Saúde
2012

Roberto Alexandre dos Santos Dias

Fosforilação da PPA na colocalização da PPA/$G_{\alpha o}$ e ativação da STAT3

APP phosphorylation on APP/$G_{\alpha o}$ colocalization and STAT3 activation

Dissertação apresentada à Universidade de Aveiro para cumprimento dos requisitos necessários à obtenção do grau de Mestre em Biomedicina Molecular, realizada sob a orientação científica da Professora Doutora Sandra Vieira, Professora Auxiliar Convidada da Secção Autónoma de Ciências da Saúde da Universidade de Aveiro.

Este trabalho contou com o apoio do Centro de Biologia Celular (CBC) da Universidade de Aveiro, e é financiado por fundos FEDER através do Programa Operacional Factores de Competitividade – COMPETE e por Fundos nacionais da FCT – Fundação para a Ciência e a Tecnologia no âmbito dos projectos PTDC/QUI-BIQ/101317/2008, PTDC/SAL-NMC/111980/2009 e PEst-OE/SAU/UI0482/2011.

Dedicada aos meus pais por todo o apoio que me deram ao longo deste percurso

o júri

presidente

Professora Doutora Odete Abreu Beirão da Cruz e Silva
Prof. Auxiliar com Agregação, Secção Autónoma de Ciências da Saúde, Universidade de Aveiro

Professora Doutora Sandra Isabel Moreira Pinto Vieira
Prof. Auxiliar Convidada, Secção Autónoma de Ciências da Saúde, Universidade de Aveiro

Doutora Maria Gomez Lazaro
Investigadora, Universidad de Castilla - La Mancha

agradecimentos

À minha orientadora, Sandra Vieira, por toda a dedicação e ajuda que me deu não só na elaboração deste trabalho mas durante todo o meu percurso como estudante universitário.

À professora Odete da Cruz e Silva, pela oportunidade de realizar este trabalho no laboratório de Neurociências do Centro de Biologia Celular.

À minha família, pelo seu incentivo e apoio contínuo que sempre me deram.

A todos os meus colegas do CBC, em especial à Regina Cerqueira, pela grande ajuda que me deu e sem a qual não teria sido possível concluir este trabalho, e à Joana Rocha, por ter sido como uma irmã mais velha, sempre pronta a ajudar e a partilhar momentos de boa disposição.

A todos os meus amigos de Ciências Biomédicas, em especial à Maria João, à Joana Tavares, ao Bruno Pimparel, ao Rui João e ao Igor, pelos momentos de lazer e descontração que foram fundamentais para vencer o cansaço.

Aos meus amigos, em especial ao Hugo, João, Joni, Ana Isabel, Denise e Patrícia, por me fazerem lembrar que a vida não é só trabalho.

À FCT pelo financiamento dos projetos PTDC/QUI-BIQ/101317/2008 e PTDC/SAL-NMC/111980/2009.

palavras-chave

Proteína precursora de amilóide de Alzheimer (PPA); fosforilação da PPA na S655; sinalização da STAT3; proteína $G_{\alpha o}$; colocalização, neuritogénese; células SH-SY5Y

resumo

A proteína $G_{\alpha o}$ é uma das subunidades alfa da família das proteínas G heterotriméricas, proteínas envolvidas na transdução de sinais a partir recetores membranares. $G_{\alpha o}$ é principalmente expressa nos neurónios, encontrando-se localizada ao longo da membrana plasmática, incluindo nos cones de crescimento dos neurónios, onde também se encontra a Proteína Precursora de Amilóide de Alzheimer (PPA), uma proteína membranar com um papel central na doença de Alzheimer. Algumas funções semelhantes já foram atribuídas às duas proteínas, incluindo papéis na diferenciação e migração celular. A ligação da PPA à Gαo já foi descrita, o que pode indicar que a PPA modula as suas funções através da ligação e ativação da $G_{\alpha o}$. Também já foi demonstrado que uma das vias pela qual a $G_{\alpha o}$ leva à neuritogénese é a ativação do transdutor de sinal e ativador da transcrição 3 (STAT3). A $G_{\alpha o}$ liga-se ao domínio C-terminal da PPA, nos aminoácidos His^{657}-Lis^{676}, que pertencem a uma região hidrofóbica imediatamente a jusante do *sorting motif* ^{653}YTSI^{656}. Isto leva a crer que a ligação entre a PPA e a $G_{\alpha o}$ pode ser mediada pela fosforilação da PPA no resíduo Serina 655 (S655). Assim, a fosforilação da PPA poderia influenciar a ativação da $G_{\alpha o}$ e consequente sinalização via STAT3.

Neste trabalho, nós estudámos os efeitos da fosforilação da PPA e ativação da $G_{\alpha o}$ na interação funcional da PPA/$G_{\alpha o}$. Isto foi analisado por cotransfeção de células de neuroblastoma humano não diferenciadas (SH-SY5Y) com PPA-GFP selvagem ou fosfomutante (PPA com a S655 constutivamente fosforilada ou desfosforilada) e com a $G_{\alpha o}$ selvagem ou $G_{\alpha o}$ constutivamente ativa. As células foram sujeitas a ensaios de imunofluorescência e vários parâmetros foram analisados, tais como a colocalização subcelular da PPA e da $G_{\alpha o}$, o número de prolongamentos celulares e o seu comprimento, e a intensidade da STAT3 no núcleo. Toda a análise quantitativa feita nas microfotografias foi realizada no software Fiji (ImageJ). Ensaios de Western Blot também foram realizados para avaliar a influência da co-expressão da PPA e $G_{\alpha o}$ em proteínas do citoesqueleto.

Os nossos resultados mostram que a $G_{\alpha o}$ e a PPA parecem colocalizar principalmente no aparelho de Golgi e nos prolongamentos celulares. Ambas as proteínas parecem cooperar entre si e induzir alterações neuritogénicas, com a $G_{\alpha o}$ a levar principalmente a uma formação inicial dos prolongamentos e a PPA a atuar na extensão dos mesmos, num modo dependente da fosforilação da S655. Além disso, observou-se que a PPA diminui a ativação da STAT3 induzida pela $G_{\alpha o}$, devido provavelmente a um efeito de retro-inibição. Estes resultados provam que estas proteínas interagem funcionalmente e o seu potencial valor em aplicações neuritogénicas terapêuticas será estudado em maior detalhe.

keywords

Alzheimer's Amyloid Precursor Protein (APP); APP phosphorylation at S655; STAT3 signalling; $G_{\alpha o}$ protein; colocalization; neuritogenesis; SH-SY5Y cells

abstract

The $G_{\alpha o}$ protein is an alpha subunit of the heterotrimeric G proteins, a protein family vastly involved in signal transduction from membranar receptors. $G_{\alpha o}$ is enriched in the plasma membrane of neurons, including neurons growth cone, together with the Alzheimer's amyloid precursor protein (APP), a transmembranar protein with a central role in Alzheimer's Disease. A few similar functions have been attributed to both proteins, such as roles in cell differentiation and migration. APP binding to $G_{\alpha o}$ has been reported, which could indicate that APP modulates its functions by binding and activating $G_{\alpha o}$. Further, one of the pathways by which $G_{\alpha o}$ leads to neurite outgrowth is by activation of the signal transducer and activator of transcription 3 (STAT3). $G_{\alpha o}$ binds to the APP C-terminal domain, namely at amino acids His^{657}-Lys^{676}, which belong to a hydrophobic pocket localized immediately downstream the APP ^{653}YTSI^{656} basolateral sorting motif. Therefore, APP binding to $G_{\alpha o}$ may be potentially mediated by APP phosphorylation at the Serine 655 residue (S655), and thus APP phosphorylation could influence $G_{\alpha o}$ activation and STAT3 signalling.

In this work we have studied the effects of APP phosphorylation and $G_{\alpha o}$ activation in $G_{\alpha o}$/APP functional interactions. This was analysed by cotransfecting human non-differentiated neuroblastoma (SH-SY5Y) cells with either Wt or phosphomutants of APP-GFP (APP with either a constitutively phosphorylated or dephosphorylated S655) and $G_{\alpha o}$ or a constitutively active $G_{\alpha o}$ cDNA. Cells were subjected to immnofluorescence assays, and several parameters analysed, such as the subcellular colocalization of $G_{\alpha o}$ and APP, the number of cellular projections and their length, and nuclear STAT3 intensity. Every quantitative analysis done upon microphotographs was performed using the Fiji (ImageJ) software. Western blot assays were also performed to evaluate the influence of APP and $G_{\alpha o}$ co-expression in cytoskeleton-related proteins.

Our results show that $G_{\alpha o}$ and APP appear to colocalize mainly in the Golgi apparatus and in cellular projections. Both proteins appear to cooperate with each other and induce neuritogenic changes, with $G_{\alpha o}$ mainly driving an initial formation of cellular projections and APP influencing their elongation, in an APP S655 phosphorylation-dependent manner. Moreover, APP was observed to decrease $G_{\alpha o}$-induced STAT3 activation, probably by a retro-inhibition effect upon earlier STAT3 activation. These results prove that these proteins functionally interact, and their potential value in neuritogenic therapeutic applications will be further studied.

Index

Abbreviations

AD	Alzheimer's disease
ADP	Adenosine diphosphate
AGS	Activator of protein signaling
AICD	APP intracellular C-terminal domain
APP	Alzheimer's Amyloid Precursor Protein
Aβ	Amyloid β-peptide
BACE1	β-site APP-cleaving enzyme
BSA	Bovine serum albumin
Ca^{2+}	Calcium
cAMP	Cyclic adenosine monophosphate
CBR1	Cannabinoid 1 receptor
Cdk5	Cyclin-dependent kinase 5
cDNA	Complementary deoxyribonucleic acid
CNS	Central nervous system
CTF	C-terminal fragment
DAPI	4',6-diamidino-2-phenylindole
ECL	Enhanced chemiluminescence
ER	Endoplasmic reticulum
FAD	Familial Alzheimer's disease
GAIP	Gα-interating protein
GAP	GTPase-activating protein
GAP43	Growth cone-associated protein 43
$G_{\alpha o}$ CA	Constitutively Active $G_{\alpha o}$
GDP	Guanosine diphosphate
GEF	Guanine nucleotide exchange factor
GFP	Green fluorescent protein
cGMP-PDE	Cyclic adenosine monophosphate phosphodiesterase

G protein	Guanine Nucleotide-Binding Protein
GPCR	G protein-coupled receptor
GRIN1	G protein-regulated inducer of neurite outgrowth 1
GSK-3β	Glycogen synthase kinase 3β
GTP	Guanosine triphosphate
JAK	Janus Kinase
K^+	Potassium
LB	Luria Bertani growth medium
MAPK	Mitogen-activated protein kinase
O/N	Overnight
PKC	Protein kinase C
PM	Plasma membrane
PreN	Pre-neurite
P-STAT3	STAT3 phosphorylated
PTX	Pertussis toxin
RGS	Regulators of G protein signaling
RT	Room temperature
SA APP	Constitutively Dephosphorylated S655 APP mutant
sAPP	Secreted APP
SDS	Sodium dodecylsulfate
SE APP	Constitutively Phosphorylated S655 APP mutant
SEM	Standard error of the mean
Src	Sarcoma-related tyrosine kinase
STAT	Signal transducer and activator of transcription
STAT3	Signal transducer and activator of transcription 3
TGN	Trans-Golgi network
TEMED	Tetramethylethylenediamine
WB	Western Blot
Wt APP	Wild type APP

1. Introduction

1.1. G protein-coupled receptors

The ability of cells to interact with each other or with the environment surrounding them is essential for organisms' survival. From simple bacteria to advanced multicellular eukaryotes, cells are gifted with mechanisms that enable them to receive a signal from the extracellular environment and transform it in an intracellular response, a process called signal transduction (Table 1) (Lodish, 2003; Lehninger et al., 2005).

Table 1 - Some of the signals to which cells respond. Adapted from Lehninger et al., 2005

Antigens	Light
Cell surface glycoproteins/oligosaccharides	Mechanical touch
Extracellular matrix components	Neurotransmitters
Growth factors	Nutrients
Hormones	Odorants
Development signals	Pheromones
Tastants	

One of the main mechanisms by which cells perform signal transduction is based on the activation of guanine nucleotide-binding proteins (G proteins) by G protein-coupled receptors (GPCRs). The human genome has over 800 genes that encode GPCRs, making them the largest family of transmembrane receptors. Several hormones, neurotransmitters and sensory stimuli act upon cells through GPCRs (Offermanns, 2003; Milligan and Kostenis, 2006). Each GPCR contains seven transmembrane helical regions, an extracellular N-terminus and an intracellular C-terminus (Fig. 1). Upon the binding of a ligand to a GPCR, the receptor suffers a conformational change that enables it to interact and activate a heterotrimeric G protein (Kroeze et al., 2003; Lodish, 2003).

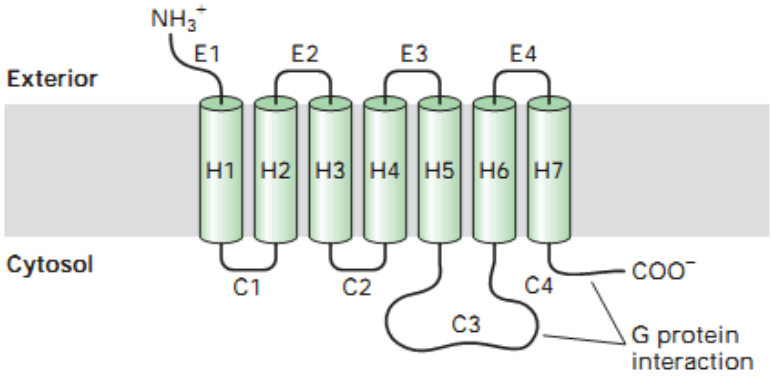

Figure 1 - Representation of a G protein-coupled receptor. Reproduced from Lodish, 2003.

1.2. Guanine Nucleotide-Binding Proteins

Heterotrimeric G proteins consist of three subunits, α, β and γ. The G_α subunit has a GTPase activity and alternates between an active state when bound to GTP and an inactive state when bound to GDP. The β and γ subunits form a single complex normally designated $G_{\beta\gamma}$ subunit (Lodish, 2003; Offermanns, 2003). While initially it was thought that only G_α interacted with the effector proteins, it is now known that both the G_α and $G_{\beta\gamma}$ are responsible for transducing the signal to their respective effector proteins (Offermanns, 2003; Milligan and Kostenis, 2006).

In an inactivated state, the G_α subunit is bound to a GDP molecule and forms a complex with the $G_{\beta\gamma}$ subunit. As aforementioned, after the binding of a ligand to a GPCR, a conformational change occurs that allows it to bind to the heterotrimeric G protein, which results in the release of GDP and binding of GTP to G_α. This reaction results in the dissociation of G_α from $G_{\beta\gamma}$, allowing both subunits to interact and modulate the activity of several effector proteins. G proteins remain active only for short periods of time due to the intrinsic GTPase activity of G_α, which hydrolyzes GTP to GDP, leading to the reassociation of G_α with $G_{\beta\gamma}$, returning the G protein to its inactive form (Fig. 2) (Kroeze et al., 2003; Offermanns, 2003; Milligan and Kostenis, 2006).

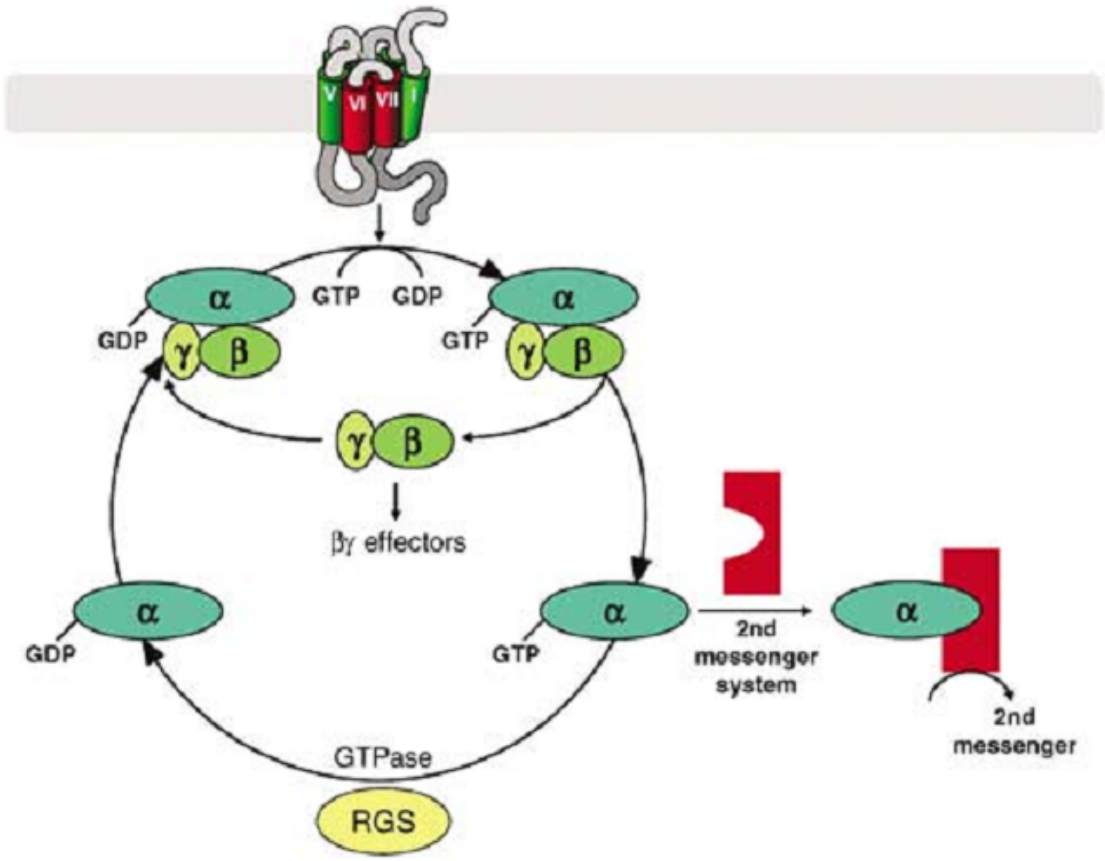

Figure 2 - The G protein activation/deactivation cycle. Reproduced from Milligan and Kostenis, 2006.

1.2.1 G proteins families

Several mammalian genes that codify G_α subunits have already been identified, 16 of which are present in humans (Gomperts et al., 2009). Since the main properties of G proteins are related to their α subunits, these have been used to divide G proteins in four subfamilies according to their functional and structural homologies: $G_{i/o}$, G_s, $G_{q/11}$ and $G_{12/13}$ (Table 2) (Offermanns, 2003; Jiang and Bajpayee, 2009).

The main members of the $G_{i/o}$ family are G_i proteins. These type of G proteins have an inhibitory effect on adenylyl cyclase activity (hence G"$_i$"), preventing it to catalyze the formation of the second messenger cAMP and thus affecting processes within the cell (Offermanns, 2003; Lehninger et al., 2005; Jiang and Bajpayee, 2009). G_t (transducin) and G_{gust} (gustducin) proteins are also members of the $G_{i/o}$ family and are involved mainly in visual and taste functions, respectively (Offermanns, 2003; Milligan and Kostenis, 2006). The G_o protein, which also belongs to this class, will be discussed further ahead.

The G_s family members have the primary function of activate adenylyl cyclases ("stimulatory"), leading to the production of cAMP. G_s and G_{olf} are the main members, with G_s being ubiquitously expressed and G_{olf} (olfactory) being mainly expressed in olfactory sensory neurons and in the central nervous system (Simonds, 1999; Offermanns, 2003).

The $G_{q/11}$ proteins are widely expressed in humans and act as mediators in the regulation of phospholipase C β-isoforms. These proteins, unlike $G_{i/o}$, are insensitive to the action of *pertussis* toxin (PTX), a protein that catalyzes ADP-ribosylation of the $G_{\alpha i}$ and $G_{\alpha o}$ subunits, rendering them incapable of performing their normal functions (Offermanns, 2003; Milligan and Kostenis, 2006; Locht et al., 2011).

The G_{12} and G_{13} are also widely expressed in human cells, although the receptors by which they are activated and the effectors with which they interact are not yet fully understood. Studies with constitutively active forms of both G proteins have led to the implication of these proteins in cell proliferation, morphology and cadherin-mediated signalling (Riobo and Manning, 2005; Milligan and Kostenis, 2006).

There are also different β and γ subunits (5β and 12γ have already been identified). Even though the βγ subunits have important functions in transducing signals, the different combinations between both subunits do not appear to affect their action, nor do the combination between different α and βγ subunits, although this has not been tested well enough. Since there are a few significant differences between some of the subunits, there is reason to believe that they may have different functions. Also, not all possible combinations are present in every cells (Offermanns, 2003; Milligan and Kostenis, 2006).

Table 2 - G_α subunits genes, expression patterns and known effectors. Adapted from Offermanns, 2003; Milligan and Kostenis, 2006.

Name	Gene	Expression	Effector/Action
$G_{i/o}$ Family			
G_{i1}	*Gnai1*	Widely distributed	Adenylyl cyclases and Ca^{2+} channels decreased function; K^+ channels and GTPase of tubulin increased function
G_{i2}	*Gnai2*	Ubiquitous	
G_{i3}	*Gnai3*	Widely distributed	
G_o	*Gnao*	Neuronal, neuroendocrine	Ca^{2+} channels decreased function; K^+ channels increased function, Adenylyl cyclases inhibition (exclusive of $G_{\alpha o-2}$ isoform)

G_z	*Gnaz*	Neuronal, platelets	Ca^{2+} channels decreased function; K^+ channels increased function
G_{gust}	*Gnag*	Taste cells, brush cells	Not known
G_{t1}	*Gnat1*	Retinal rods, taste cells	cGMP-PDE increased function
G_{t2}	*Gnat2*	Retinal cones	
G_s Family			
G_s	*Gnas*	Ubiquitous	Adenylyl cyclases, Src tyrosine kinases, GTPase of tubulin increased;
G_{olf}	*Gnal*	Olfactory neurons, brain	Adenylyl cyclases increased
$G_{q/11}$ Family			
G_q	*Gnaq*	Ubiquitous	Phospholipase Cβ isoforms and K^+ channels increased function
G_{11}	*Gna11*	Almost ubiquitous	p63-RhoGEF increased function
G_{14}	*Gna14*	Kidney, lung, spleen	Not known
G_{16}	*Gna15*	Hematopoietic cells	
$G_{12/13}$ Family			
G_{12}	*Gna12*	Ubiquitous	Phospholipase D and Cε increased function; E-cadherin-mediated cell adhesion increased
G_{13}	*Gna13*	Ubiquitous	

1.2.2. Modulators of G protein activity

The activation/deactivation cycle of G proteins can be regulated by several proteins that can be divided into two groups: Regulators of G-protein Signalling (RGS) and guanine nucleotide exchange factors (GEFs) (Fig. 3).

RGS have over 30 intracellular proteins already discovered. These can modulate G protein activity mainly by increasing their rate of hydrolysis of GTP by the G_α subunit and thus inactivating G proteins more quickly. Because of this function, RGS proteins are also called GTPase-activating proteins (GAPs), however this designation is used more often to describe the proteins that have this same function but interact with small monomeric G proteins, like Ras (Gomperts et al., 2009). Besides GAP activity, RGS proteins can physically block the interaction between G_α and effector proteins, and increase the affinity of G_α to $G_{\beta\gamma,}$ which leads to rapid reassembling of the heterotrimeric

form of G proteins after GTP hydrolysis, thus preventing $G_{\beta\gamma}$ subunits of interacting with their effector proteins (De Vries et al., 2000; Roman and Traynor, 2011).

GEFs are able to activate G proteins by increasing the rate of exchange of GDP by GTP. GPCRs are the most well known proteins that act as GEFs of heterotrimeric G proteins (De Vries et al., 2000; Jiang and Bajpayee, 2009).

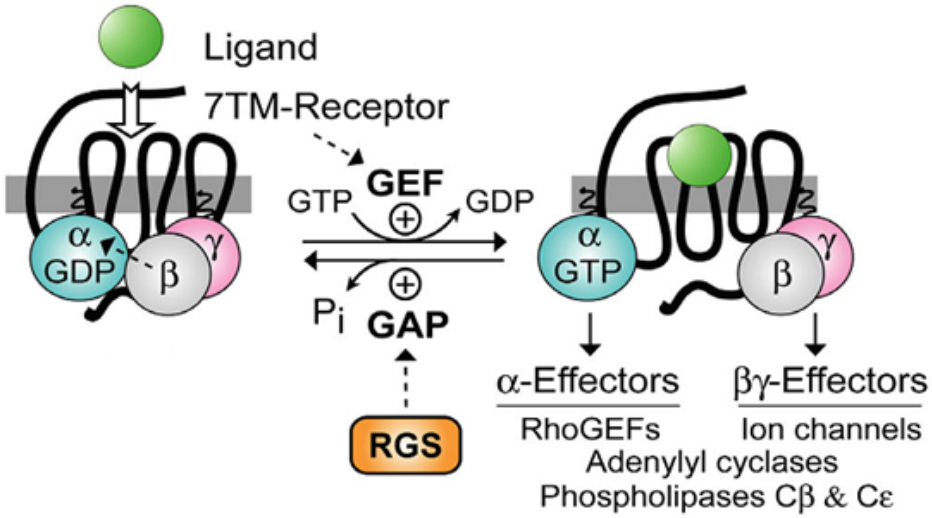

Figure 3 - Modulation of G proteins action by Regulators of G-protein signalling (RGS) and guanine nucleotide exchange factors (GEFs). Reproduced from Siderovski and Willard, 2005

1.3. The Other Guanine Nucleotide-Binding Protein

The G_o protein is the most expressed G protein in the central nervous system, where it accounts for about 1% of total membrane protein. It was accidentally discovered in 1984 when researchers were trying to isolate G_i protein from bovine brain and detected an extra G_α subunit with a molecular weight of 39 kDa, naming it the "other" G protein, to differentiate from G_i and G_s (Sternweis and Robishaw, 1984; Jiang and Bajpayee, 2009). Since then, it has been intensively studied and several GPCRs, among other proteins, had already been discovered to interact with G_o; however, its main functions are not yet fully understood. Being highly expressed in brain tissue, G_o as been implicated in neuronal development, migration, and such diseases as Alzheimer's and Parkinson's (Jiang et al., 1998; Jiang and Bajpayee, 2009).

1.3.1. G_o genetics

G_o protein has already been identified in several species, such as rat, mouse, bovine, *Drosophila* and human, among others. Comparison between DNA sequences of the different G_o genes showed that this protein is highly conserved across species, which suggests that G_o signalling is extremely important for organisms to receive, integrate and execute extracellular signals (Murtagh et al., 1991; Jiang and Bajpayee, 2009).

The human $G_{\alpha o}$ gene comprises over 100 kb and contains 11 exons, being localized in chromosome 16 (Tsukamoto et al., 1991). Analysis of bovine and mouse brains have led to the discovery of two isoforms of $G_{\alpha o}$, $G_{\alpha o\text{-}1}$ and $G_{\alpha o\text{-}2}$ (also called $G_{\alpha o\text{-}A}$ and $G_{\alpha o\text{-}B}$), which were later found in human cells. Both isoforms are identical in the first two thirds of the amino acid sequence, differing only in 20 amino acids in the latter third of the protein. Study of the human gene found that the exon 8 and 9 are duplicated, and that $G_{\alpha o\text{-}1}$ contains exon 7-A and 8-A while $G_{\alpha o\text{-}2}$ contains exon 7-B and 8-B. This indicates that both isoforms are a product of alternative splicing, and since exon 7 and 8 are thought to be necessary to receptor and effector binding, these isoforms may have different functions in the human brain (Lang, 1989; Hsu et al., 1990; Tsukamoto et al., 1991; Jiang and Bajpayee, 2009).

1.3.2. Modulators of G_o activity

Being a member of the $G_{i/o}$ family, G_o suffers ADP-ribosylation by PTX in its carboxyl terminal cysteine residue of the α subunit, inactivating it (Jiang and Bajpayee, 2009; Locht et al., 2011). A few RGS proteins have been identified that accelerate the process of G_o inactivation, being one of those proteins the G_α-interacting protein (GAIP). This protein has been found to specifically interact with G_o, only losing that specificity when its N-terminal was deleted (Diverse-Pierluissi et al., 1999; Jiang and Bajpayee, 2009).

Several GPCRs that are able to exert their action trough G_o proteins have already been identified, including opioid, α_2-adrenergic, M2 muscarinic and somatostatin receptors (Jiang et al., 1998). All of these act as GEFs, causing G_o to dissociate from GDP and bind GTP. Beside GPCRs, other molecules have been identified that activate

G_o, such as the growth cone-associated protein with a molecular weight of 43 kDa (GAP43), the activator of G protein signalling (AGS), the Presenilin I enzyme and the Alzheimer's Amyloid Precursor Protein (APP) (Jiang and Bajpayee, 2009). GAP43, a protein expressed in developing neurons, is thought to act upon G_o in a manner similar to GPCRs. However its action is not affected by the presence of PTX or the βγ subunit, which leads to the believe that is mechanism of action is somehow different of other GEFs (Strittmatter et al., 1991; Jiang and Bajpayee, 2009). AGS studies in vitro showed that this protein enhanced $GTP_{\gamma}S$ binding to both G_i and G_o (Cismowski et al., 2000). A physical interaction between Presenilin I and G_o has been described, which led to the possibility of this protein performing its functions through G_o. Besides that, the interaction of the two proteins could also be implicated in Alzheimer's disease (Smine et al., 1998; Jiang and Bajpayee, 2009). The interaction between G_o and APP will be discussed in more detail further ahead.

Other factors have also been identified that interact and possibly modulate G_o activity. However, their exact mechanism and effect are not fully comprehended. Such is the case of GoLoco motif, a 19 amino acid sequence originally found in the RGS12 protein that binds to $G_{\alpha o}$, though is not known whether it acts as a GEF or rather decreases G_o activity by stabilizing it in the GDP-bound form (Siderovski et al., 1999; Jiang and Bajpayee, 2009).

1.3.3. G_o expression pattern

G_o protein is expressed mainly in the central nervous system (CNS), however, its distribution along the brain does not appear to be equal. Immunohistochemical studies in rat brains showed that G_o is highly present in the cerebral cortex, cerebellum, hypothalamus, hippocampus and substantia nigra, being located mainly in the cytoplasmatic face of the plasma membrane, including cell-to-cell contacts (Worley et al., 1986; Gabrion et al., 1989). Besides CNS, G_o has also been located in the heart tissue, pituitary gland and pancreatic isles (Wolf et al., 1998; Jiang and Bajpayee, 2009).

G_o expression was also studied in different stages of neuronal differentiation. In undifferentiated neuroblastoma x glioma hybrid cells, G_o levels were very low but after these cells suffered differentiation, G_o levels significantly increased. Besides that, only

G_{o2} isoform is expressed in undifferentiated cells, whereas both G_{o1} and G_{o2} were expressed in differentiated cells, a factor that contributes to the increase in G_o protein levels (Mullaney and Milligan, 1989; Brabet et al., 1991).

1.3.4. G_o functions

The G_o protein seems to have several functions mediated through a large number of effector molecules. Most of those functions involve the modulation of ion channels, kinases activity and vesicular transporters (Jiang and Bajpayee, 2009).

Calcium channels: Several neurotransmitters and hormones that inhibit voltage-gated Ca^{2+}, such as noradrenaline and somatostatine, have been known to act through GPCRs. Initial studies using PTX on neurons led to the discover that the inhibitory effect of the neurotransmitter over the calcium channels was lost when the toxin was present, which suggested that PTX-sensitive G proteins, such as Gi and Go, were involved (Holz et al., 1986; Hille, 1994; Jiang and Bajpayee, 2009). Further studies using antibodies specific for the $G_{\alpha o}$ subunit showed that the inhibitory effect of noradrenaline was diminished when the antibodies were applied (Caulfield et al., 1994).

Potassium channels: Like in the calcium channels, there are neurotransmitters that interact with K^+ channels through PTX-sensitive G proteins. Experiments using membranes of hippocampal pyramidal cells allowed to identify four K^+ channels that were activated by purified G_o proteins and a recombinant $G_{\alpha o}$ subunit (VanDongen et al., 1988; Jiang and Bajpayee, 2009).

The activation of K^+ channels by G_o was also studied in the heart muscle and peripheral neurons. However the results showed that it was the $\beta\gamma$ subunit of the heterotrimeric complex rather than the α subunit that interacted and activated the K^+ channels (Huang et al., 1997; Lei et al., 2000).

Besides potassium and calcium channels, G_o also appears to be involved in the regulation of sodium channels, however the receptors involved in this pathway have not yet been identified (Jiang and Bajpayee, 2009).

MAPK pathway: several studies indicate that G_o is involved in the activation of the mitogen-activated protein kinase (MAPK) pathway (Jiang and Bajpayee, 2009). For example, one of those studies demonstrated that a constitutively active $G_{\alpha o}$ was able to activate B-Raf in a Protein Kinase C (PKC)-dependent manner and consequently stimulate the MAPK pathway (Antonelli et al., 2000).

STAT3 pathway: The signal transducer and activator of transcription 3 (STAT3) is a known proto-oncogenic protein that is involved in the development of several cell lines, from hematopoietic cells to neurons. It was recently found that STAT3 can be activated by receptors coupled to G_o (He et al., 2005; Hankey, 2009). One of those receptors is the cannabinoid receptor (CBR1), which, when activated, leads to the stimulation of the STAT3 pathway. This mechanism appears to involve the direct interaction between G_o and regulators of small monomeric G proteins, such as Rap1 and its GAP protein, that are present in the STAT3 pathway. This results in the activation of Scr tyrosine kinase, culminating in the phosphorylation of STAT3 (Fig. 4). This G_o-signalling was observed in Neuro-2A cells, which led to neurite outgrowth (He et al., 2005).

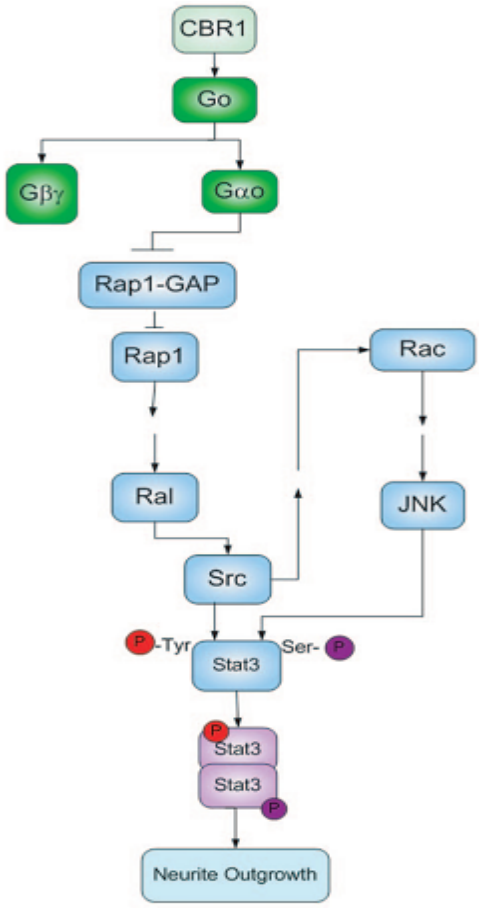

Figure 4 - STAT3 Pathway leading to neurite outgrowth. Reproduced from He et al., 2005

Vesicular transporters: G_o proteins are present in both secretory granules and small synaptic vesicles in bovine and rat brain. The exact mechanism in which G_o is involved in these structures is still not well known, however a few possible functions have been proposed. One of those is the control of the uptake of neurotransmitters, since activation of G_{o2} inhibits the uptake of noradrenaline in PC12 cells (Ahnert-Hilger et al.,

1994; Ahnert-Hilger et al., 1998). It was also demonstrated that G_o interacts with small G proteins (Rho) in a mechanism necessary for the reorganization of neurons cytoskeleton in the exocytosis process (Jiang and Bajpayee, 2009).

G_o protein seems to have significant importance in the brain due to its abundance in this tissue. Studies in mice lacking G_o revealed that the absence of the protein led to severe motor control deterioration, hyperactive behaviour and hyperalgesia (Jiang et al., 1998). The molecular role of G_o in the brain has been studied and its interaction, directly or indirectly, with other brain proteins have led to the discovery of a few specific roles. One of those signalling pathways has already been described above, the STAT3. Another one is the Growth Associated Protein 43 (GAP-43), a protein highly expressed in the growth cones of developing and regenerating neurons, which indicates that it may be involved in neurite growth (Strittmatter et al., 1991; Strittmatter et al., 1994). Like stated above, GAP-43 is a known GEF for G_o protein, leading to the believe that GAP-43 is able to modulate neurite growth and motility through G_o activation. Strittmatter et al have already produced some results that indicate just that. In their studies, GAP-43 was shown to increase neurite outgrowth by stimulating G_o in neuroblastoma cells (Strittmatter et al., 1994). Another study using constitutively activated $G_{\alpha o}$ (a mutated $G_{\alpha o}$ lacking its GTPase activity) showed that increase in neurite outgrowth could be caused by inhibition of PKC and modulation of intracellular calcium release (Xie et al., 1995).

Another important role of G_o in the brain appears to be its involvement in Alzheimer's Disease, an hypothesis that arrived with the discovery that G_o interacts with the Alzheimer's Amyloid Precursor Protein (Nishimoto et al., 1993).

1.4. The Alzheimer's Amyloid Precursor Protein

Alzheimer's Amyloid Precursor Protein (APP) is a transmembrane protein mainly present in the Golgi and plasma membrane of neuronal cells. Its specific functions are still not very clear, but it is thought to be involved in cell adhesion signalling, neurite outgrowth and synaptic contact, being also the precursor protein of β-amyloid (Aβ) (Small, 1998; Thinakaran and Koo, 2008). The Aβ peptide is the main

component of amyloid plaques (also called senile plaques), one of the main features of Alzheimer's Disease (AD), and it has been associated to most of the pathological changes that occur during the progress of AD, such as induction of inflammatory reactions, neuronal dysfunction, synapse loss and cell death (Hardy and Higgins, 1992; Sommer, 2002; Henriques et al., 2010). Its production depends on the processing of APP, a process that will be explained further ahead.

APP arises from the expression of a gene located in the chromosome 21. There are several isoforms resulting from alternative splicing, with APP695 being the most common in the brain (the number represents the amino acids content of the protein) (Fig. 5). APP has only one transmembranar domain, with most of the protein being located in the extracellular space and just a small C-terminal domain being located in the intracellular space (Small, 1998; Ling et al., 2003). After its expression, APP suffers several post-translational modifications that are essential for its function, such as glycosylation and phosphorylation.

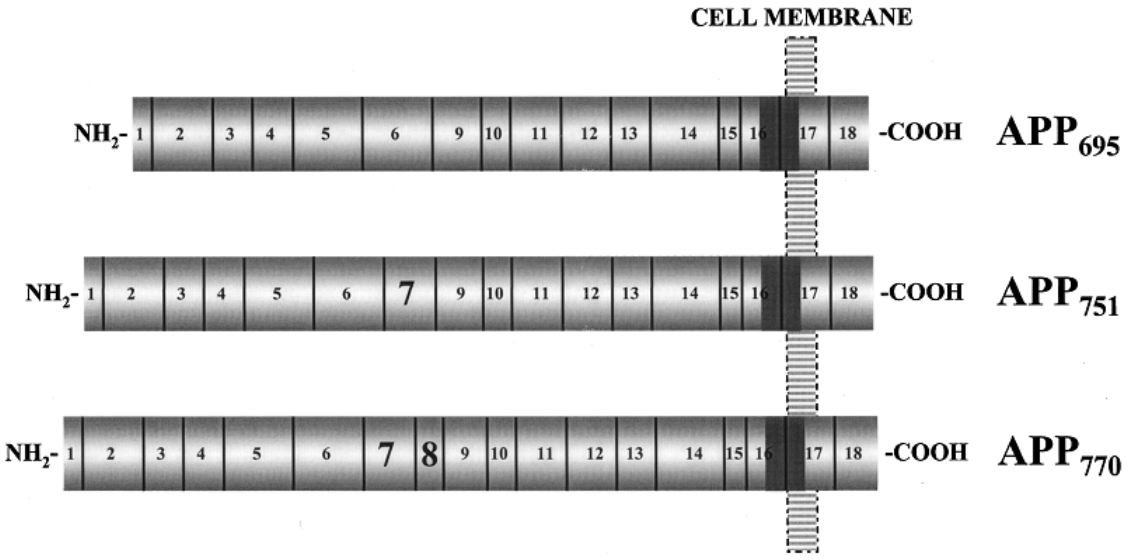

Figure 5 - Different isoforms of APP. Reproduced from Edgar F. da Cruz e Silva and Odete A. B. da Cruz e Silva, 2003

1.4.1. APP processing

APP can be cleaved by several secretases, giving rise to some peptides with important physiological and pathological function. Those secretases are mainly divided in α, β and γ secretases and depending on which of these cut APP, Aβ may or may not be generated (Figure 6). γ-secretase cuts the APP transmembrane domain on several sites. Its action gives rise to AICD (APP intracellular domain), a peptide that has been implied in a few signalling pathways. AICD can bind to Fe65, which results in the formation of a complex responsible for the activation of the transcription of several genes, including p53, GSK-3β, Kai1, among others. However, the precise mechanism by which AICD binding to Fe65 leads to gene transcription is not well known (Ling et al., 2003; Thinakaran and Koo, 2008; Chow et al., 2010).

The action of the other two secretases defines the processing pathway of APP. In the non-amyloidogenic pathway (Fig. 6 - left), α-secretase cuts APP in the Aβ region, generating secreted APPα (sAPPα) and a C-terminal fragment (α-CTF), the latter being then cleaved by the γ-secretase, originating the p3 fragment and AICD. In this pathway, no Aβ is generated (hence non- amyloidogenic), which is why this process is normally dubbed neuroprotective. Further, the formation of sAPPα also contributes to the neuroprotective function of the non-amyloidogenic pathway. The precise mechanisms

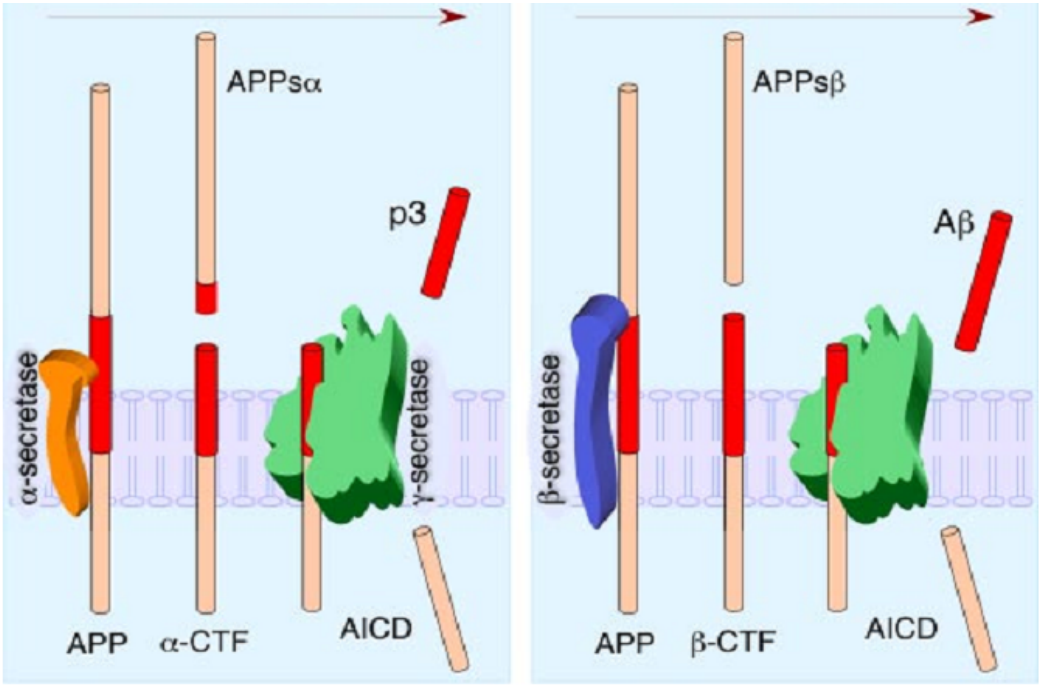

Figure 6 - Non-amyloidogenic (left) and amyloidogenic pathway (right). Reproduced from Thinakaran and Koo, 2008

in which sAPPα is involved are not fully understood, but studies indicate that it promotes neurite outgrowth, synaptogenesis and cell adhesion, and protects neurons against oxygen deprivation and excitotoxicity (Ling et al., 2003; Gakhar-Koppole et al., 2008; Chow et al., 2010). No function as yet been assigned to the non pathogenic p3 fragment (Ling et al., 2003).

On the other hand, the cut of APP by the β-secretase is termed amyloidogenic pathway (Fig. 6 - right). The β-secretase cuts APP in its β-cleavage site, generating sAPPβ and C99 (or β-CTF). The C99 is then cleaved by γ-secretase, giving rise to Aβ (hence amyloidogenic) and AICD. The main β-secretase involved in this pathway is BACE1 (β-site APP-cleaving enzyme 1). The sAPPβ has still not a clear function (Ling et al., 2003; Cole and Vassar, 2008; Chow et al., 2010).

1.4.2. APP trafficking

The first steps in APP post-translational modification are its N- and O-glycosylation, followed by its phosphorylation and tyrosine sulfation. These occur during its transport from the endoplasmic reticulum to the plasma membrane (Figure 7, step 1). However, only a small portion of the expressed APP is localized to the plasma membrane. Most of it remains in the Golgi apparatus or in the Trans-Golgi network (TGN) (Thinakaran and Koo, 2008; Zheng and Koo, 2011).

In the plasma membrane, APP can suffer non-amyloidogenic processing, due to the presence of the α-secretase in the membrane. On the other hand, shortly after its integration in the membrane, APP is internalized by endocitosis (Figure 7, step 2) and can either be degraded in lysosomes or recycled back to the membrane (Fig. 7, step 3). During this transport, APP comes in contact with BACE1 in several compartments, such as the endosome and the TGN. This promotes the amyloidogenic processing of APP and consequently Aβ generation. It has been shown that several proteins, like Fe65, interact with the APP C-terminal and modulate its intracellular trafficking, interfering with the production of Aβ (Small and Gandy, 2006; Thinakaran and Koo, 2008).

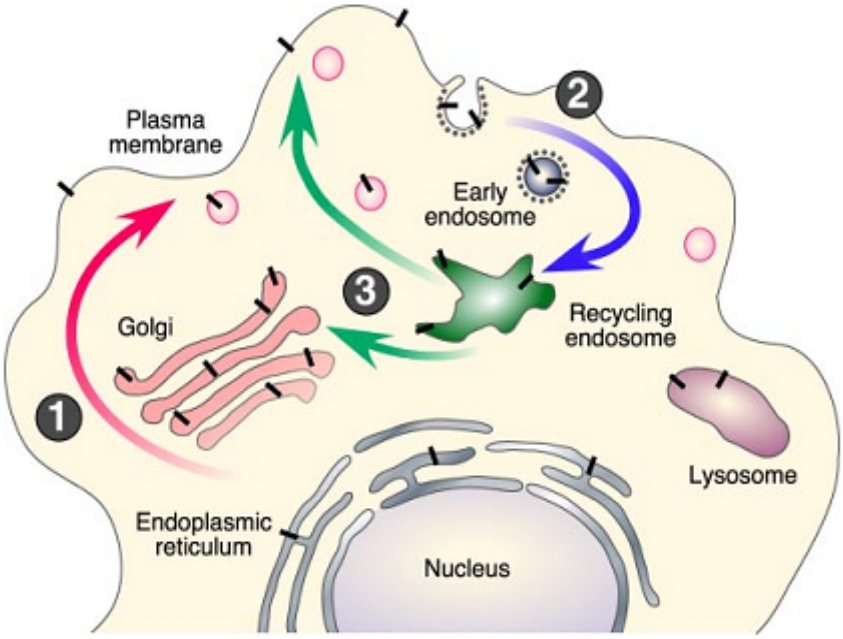

Figure 7 - APP trafficking. Reproduced from Thinakaran and Koo, 2008

1.4.3. APP phosphorylation

The processing, trafficking and function of APP is regulated in many ways, with phosphorylation appearing to have an important part in all of these processes. A few phosphorylation sites have been identified in both the intracellular and extracellular domain of APP. The serines 198 and 206 are the amino acids phosphorylated in the APP ectodomain, but no relevant function have been so far attributed to these phosphorylations (Walter et al., 1997; da Cruz e Silva and da Cruz e Silva, 2003).

On the other hand, some of the phosphorylation sites discovered in the intracellular domain of APP have a significant impact in its life. These include the Thr^{654}, Ser^{655}, Thr^{668}, Tyr^{682} and Tyr^{687}. The Thr^{668} is one of the best studied phosphorylatable amino acids of APP, being phosphorylated by GSK-3β, Cdk5 and JNK, although its role is still controversial. Thr^{668} phosphorylation has been linked to both increases and decreases in Aβ formation and in the regulation of the binding of AICD to Fe65 followed by translocation of the complex to the nucleus, or not having any effect in this process (Suzuki and Nakaya, 2008; Schettini et al., 2010).

Phosphorylation of Serine 655 (S655), present in the YTSI sorting sequence, potentially by protein kinase C, has been described as an important event in APP processing, trafficking and its interaction with other proteins. A study using APP phosphomutants mimicking a constitutively phosphorylated and a constitutively

dephosphorylated S655 (S655E and S655A, respectively) showed that S655 phosphorylation increased APP trafficking through the Golgi to the plasma membrane, and an increase in sAPPα production. The two events are most likely related since the continuous trafficking of APP renders it more available to α-secretase cleavage (Vieira et al., 2009). Another study showed that S655 phosphorylation leads to an increase in APP recycling through a retromer mediated process. It also decreases APP targeting to lysosomes, thus expanding its half-life (Vieira et al., 2010).

Interestingly, the binding of APP to $G_{\alpha o}$ (discussed in more detail further ahead) occurs immediately downstream of the sorting motif ^{653}YTSI^{656}, which can indicate that APP S655 phosphorylation may influence the interaction between both proteins.

1.5. G_o binding to APP

APP was found to selectively bind to $G_{\alpha o}$, but not $G_{i\alpha}$, through APP His^{657}-Lys^{676} domain, and described to activate $G_{\alpha o}$ (Nishimoto et al., 1993). Further studies involving phospholipid vesicles containing both APP695 and G_o identified APP as a GPCR-like protein, with a possible natural ligand not yet identified but who's action was mimicked by 22C11, an antibody directed against the extracellular domain of APP. When the antibody bound to APP, G_o activation was greatly enhanced due to an increase in the GDP/GTP exchange rate. The ability of APP695 to activate G_i in the presence of 22C11 was also tested, with negative results, indicating that APP binds specifically to G_o protein (Okamoto et al., 1995).

A more recent study shed a new light in the mechanism by which APP activates G_o. This study also evaluated the action of the 22C11 in the interaction of APP to Go, however the results showed a decrease in the GTPase activity of G_o, a phenomenon not detected in the earlier study. The authors attributed this difference of results to the fact that the study conducted by Okamoto et al, was done using phospholipid vesicles, which probably lack a few cofactors needed to the decrease in the G_o GTPase activity. Since this decrease would make G_o active for longer periods of time, this could be an alternative mechanism by which APP increases the activity of G_o proteins. However, this is not yet certain, with further research being required (Brouillet et al., 1999).

1.5.1. G_o:APP and Alzheimer's Disease

Mutations in the APP gene have already been identified in cases of genetic-linked Familial Alzheimer's Disease (FAD). One class of specific mutations is the V642, where the valine at the 642 position is mutated into isoleucine (V642I), phenylalanine (V642F) or glycine (V642G) (Hardy, 1992; Karlinsky et al., 1992). All these mutations were shown to cause apoptosis in COS-NK1 cells in a G_o-mediated mechanism, since knockout of G_o, but not G_i, led to the suppression of apoptosis (Fig. 8). G_o involvement was also tested by transfecting COS cells with V642-APPs mutants lacking the His^{657}-Lys^{676} sequence. In these cells, apoptosis was also greatly diminished in comparison with V642-APPs mutants, giving stronger evidences of the mediating function of G_o in APP-induced apoptosis (Yamatsuji et al., 1996). To clarify which of the G_o subunits was responsible for the activation of the apoptosis cascade, a series of tests were made in NK1 cells involving constitutively activated $G_{\alpha o}$ (Q205L) and βARK1 C-terminus, a binding site to $G_{\beta\gamma}$ subunits that inhibits its functions. The results showed that constitutively activated $G_{\alpha o}$ induced little apoptosis while βARK1 C-terminus inhibited NK1 apoptosis, leading to the conclusion that $G_{\beta\gamma}$ subunit, and not G_α, was responsible for triggering apoptosis (Giambarella et al., 1997).

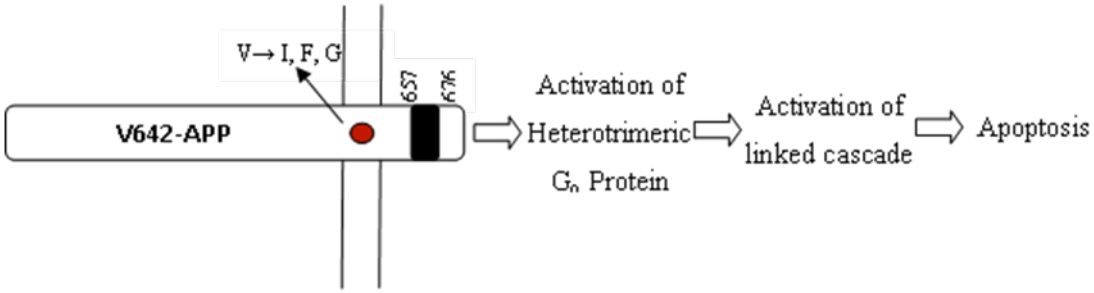

Figure 8 - Mediation of V642-APP-induced apoptosis by G_o protein. Adapted from Yamatsuji et al, 1996

1.5.2. APP and $G_{\alpha o}$ in neuritogenesis

Since some of the functions of APP have also been attributed to the G_o protein, it was hypothesized that APP could mediate its functions through G_o, acting most likely as a $G_{\alpha o}$ GEF (Nishimoto et al., 1993; Okamoto et al., 1995; Okamoto et al., 1996).

One of those functions is neuritogenesis. As stated above, $G_{\alpha o}$ induction of neurite outgrowth has already been described via STAT3 pathway. A different pathway

by which $G_{\alpha o}$ could lead to neurite growth is by activation of the G Protein-Regulated Inducer of Neurite Outgrowth 1 (GRIN1) (Nakata and Kozasa, 2005), however in this work we will focus on the STAT3 pathway.

APP role on neuritogenesis has also been described. Initial studies showed that APP expression increased neurite length and branching in PC12 cells, possibly by mediating the Nerve Growth Factor action (Milward et al., 1992). Another study analyzed the effect of down-expression of APP on neuronal primary cultures. The results indicated that the blockage of APP expression leads to a decrease in axon and dendritic growth (Allinquant et al., 1995).

More recent studies indicate that while APP clearly influences neuritogenesis, it may have an inhibitory effect rather than stimulatory. Also, sAPPα seems to be fundamental to regulate APP function. In one of those studies, loss of APP expression in primary neuronal culture culminated in increased neurite elongation, with this same result occurring when sAPPα was applied to the cells expressing APP. Both these effects were blocked with the use of antibodies directed against Integrin β1. The hypothesis defended was that full-length membranar APP is able to interact with Integrin β1 leading to the inhibition of neurite outgrowth, while sAPPα blocks this interaction and thus allows neurite elongation (Young-Pearse et al., 2008).

Previous work developed in our lab was dedicated to understanding the role of APP in neuronal differentiation (Rocha, 2011). The study was conducted in SH-SY5Y cells and showed that while long-term overexpression of APP could have a negative effect on neuritogenesis, short-term expression (24h) leads to an increase in neurite outgrowth. Also, with the use of phosphomutants APP-GFP cDNAs, the positive neuritogenic action of APP was found to be enhanced by APP S655 phosphorylation.

2. Aims

This work focused on characterizing the interaction between the Alzheimer's Amyloid Precursor Protein and $G_{\alpha o}$ protein, with its main aims being:

- To evaluate the effects of APP S655 phosphorylation and $G_{\alpha o}$ constitutive activation in APP-$G_{\alpha o}$ colocalization in SH-SY5Y cells.
- To study the effect of APP-$G_{\alpha o}$ co-expression in the induction of cellular morphological changes, and how APP phosphorylation and $G_{\alpha o}$ activation regulate that effect(s).
- To analyse the impact of $G_{\alpha o}$ and APP co-expression in cytoskeleton-related proteins.
- To evaluate the effect of APP phosphorylation in $G_{\alpha o}$-induced STAT3 activation.

3. Methods

3.1. Wild type (Wt) and S655 Phosphomutants APP-GFP cDNAs

APP cDNAs, S655 point mutated and fused to GFP (Green Fluorescent Protein) were already available at the lab. Briefly, human APP isoform 695 cDNA was used as a template to generate S655 cDNA point mutations, namely Serine 655 to Alanine (S655A) or to Glutamate (S655E), using site-directed mutagenesis. Due to their structure, these amino acids mimic a constitutively phosphorylated (Glutamate) and dephosphorylated (Alanine) S655. These mutants, together with parental Wt cDNA, were subcloned into the pEGFP-N1 vector (Clontech), a plasmid that encodes GFP. The result was a fusion gene of APP with GFP in its N-terminal (Vieira et al., 2009).

3.2. Wt and Constitutively Active $G_{\alpha o}$ cDNAs

The human $G_{\alpha o}$ cDNAs were acquired from the Missouri S&T cDNA Resource Center. The $G_{\alpha o}$ subunit open reading frame (isoform $G_{\alpha o\text{-}1}$) had been amplified from human whole brain cDNA (Clontech) by PCR and subcloned into pcDNA3.1+ vector (Invitrogen) between Kpn I (5') and Xba I (3') restriction sites. The Constitutively Active $G_{\alpha o}$ ($G_{\alpha o}$ CA) had been engineered by substituting Glutamine 205 by a Lysine (Q205L), using the Quickchange mutagenisis kit (Stratagene). This substitution significantly reduces the GTPase activity of $G_{\alpha o}$, rendering it constitutively active. Both $G_{\alpha o}$ inserts have a size of 1070 bp.

3.3. $G_{\alpha o}$ and constitutively active $G_{\alpha o}$ cDNAs amplification and purification

3.3.1. Bacterial transformation

E. Coli XL1-Blue competent cells were thawed on ice and 0,25 µg (5 µL) of $G_{\alpha o}$ and $G_{\alpha o}$ constitutively active cDNAs were each added to a 100 µl aliquot of competent cells. The cells were incubated on ice for 30 min. After this, they were subjected to an heat shock by incubation in a 42 ºC bath for 90 sec and then rapidly transferred to ice

for 2 min. 900 µl of SOC medium was added to the cells and a 45 min incubation at 37 ºC followed. Finally, the cells were centrifuged at 14000 rpm for 30 sec, the supernatant was discarded and the pellet was resuspended in the remaining volume (100 µL), plated onto LB/ampicillin agar plates and incubated at 37 ºC during 16-18 h.

3.3.2. MegaPrep DNA Purification

One colony of transformed bacteria with each $G_{\alpha o}$ cDNA was isolated and added to 3 mL of LB medium and incubated during 16-18 h at 37 ºC, with agitation. After bacterial growth, 1 mL of cells was transferred to 1 L of LB medium and again incubated overnight (O/N) at 37ºC with agitation. Cells were then centrifuged at 1500 x g, for 20 min (Beckman Avanti J-25 I - Beckman Coulter), the supernatant discarded and 30 mL of Cell Resuspension Solution was added. After resuspension, 30 mL of Cell Lysis Solution was added and mixed. After the solution became clear and viscous, 30 mL of Neutralization Solution was added, mixed and centrifuged at 20000 x g for 15 min. The supernatant was filtered using filter paper and the remaining volume was measured. 0,5 volume of isopropanol was added and then centrifuged at 14000 x g for 15 min. The supernatant was discarded and the pellet was resuspended in 4 mL of sterile water. 20 mL of Wizard® Megapreps DNA Purification Resin was added to the solution and mixed. The mix was then transferred to a Megacolumn, inserted in a vacuum manifold port, and vacuum was applied. The column was then washed 2 times with Column Wash Solution, also by applying vacuum. 5 mL of ethanol 80% was added to the column and vacuum was applied. The column was then transferred to a 50 mL screw cap tube and centrifuged at 1300 x g for 5 min (Eppendorf Centrifuge 5810R). The liquid was discarded and the column was again placed in the vacuum manifold and dried by applying vacuum for 5 min. The column was then removed, placed in a new 50 mL screw cap tube, and 3 mL of pre-heated (65-70 ºC) nuclease-free water was added to the column. After 1 min, the column was centrifuged at 1300 x g for 5 min, the liquid transferred to microcentrifuge tubes (400 µL per tube) and stored at -20 ºC. This procedure had been previously done in laboratory for the APP-GFPs cDNAs

3.3.3. Ethanol precipitation of plasmid DNA

Ethanol precipitation was also performed in order to increase DNA purification, which is essential for optimal transfections. 1/10 of sodium acetate was added to each

microcentrifuge tube containing the DNA solution. 2,5 volume of ethanol 100% was further added, mixed and incubated O/N at -20 ºC. After, the tubes were centrifuged (14000 x g, 15 min, 0 ºC), the supernatant discarded and 750 µL of ethanol 70% (half of the tube capacity) was added and mixed. The solutions were incubated during 5 min, at -20 ºC, and then centrifuged (14000 x g, 5 min, 0 ºC). The supernatant was discarded and the pellet was dried. After all traces of ethanol disappeared, the DNA in each tube was resuspended in 200 µL of sterile water and stored at -20ºC.

3.4. Culture and maintenance of the SH-SY5Y cell line

The SH-SY5Y human neuroblastoma cells are derived from the SK-N-SH cell line, originally established from a bone marrow biopsy of a neuroblastoma patient. The SH-SY5Y cells were maintained in a 10% FBS MEM:F12 (1:1) growth medium, in a 5% CO_2 humidified incubator at 37 ºC. Cells were divided when they reached 70-80% confluence, and transfected with the appropriated cDNAs as follows.

3.5. Transfection of the SH-SY5Y cell line with APP-GFP and $G_{\alpha o}$ cDNAs

In order to be able to study the effects of APP phosphorylation and $G_{\alpha o}$ activity in cells, Wt and CA $G_{\alpha o}$ cDNAs, along with Wt, S655A and S655E APP-GFP cDNAs, were transfected into SH-SY5Y cells. Three different transfection reagents were first tested in order to optimize SH-SY5Y cells transfection: jetPRIME® (Polyplus-transfection), TurboFect™ (Fermentas Life Sciences) and CombiMag™ (OZ Biosciences). For each of the reagents used, cells were seeded in 6-well plates 24 h before transfection, so that cells could be around 80 to 90% at the time of transfection. Also, the growth medium was changed immediately before the transfection procedure.

3.5.1. JetPRIME® transfection

The jetPRIME® transfection reagent is a molecule based on a non-liposomal formulation produced by Polyplus-transfection™. For each well, 1 µg of cDNA was diluted in 100 µL of jetPRIME® buffer. Then, 2 µL jetPRIME® reagent was added,

vortexed and the mix was incubated for 10 min at room temperature (RT). After this, the mixture was added to each well and mixed by gently agitating the plate. The cells were then incubated at 37 ºC in a 5% CO_2 incubator. After 4 h, the cell medium was changed, and 24 h after transfection cells were collected in 250 µL 1% SDS for Western Blotting (WB).

3.5.2 TurboFect™ transfection

The TurboFect™ transfection reagent is a cationic polymer that forms a positively charged complex with DNA that is easily endocytosed by eukaryotic cells. Briefly, for each well, 1 µg of cDNA was diluted in 100 µL of serum-free growth medium. After gently vortexing it, 2 µL of TurboFect™ reagent was added to the DNA, mixed and incubated during 15 min at RT. It was then added to each well and mixed by gently agitating the plate. The cells were incubated at 37 ºC in a 5% CO_2 incubator. After 6 h, the cell medium was changed, and at 24 h of total transfection time, cells were collected in 250 µL 1% SDS for WB.

3.5.3 CombiMag™ transfection

CombiMag™ transfection reagent is a solution containing magnetic particles that is used in combination with any other transfection reagent to improve its efficiency. In this case it was used in combination with TurboFect™. It uses the principle of Magnetofection™, in which magnetic particles associate with vectors and then come into contact with cells by applying a magnetic force, thus enhancing the transfection efficiency (Scherer et al., 2002). First, for each well, 1 µL of CombiMag™ reagent was transferred to a microtube. Then, the TurboFect™ mixture was prepared by mixing 1 µL of the reagent to 1 µg of DNA in a microtube containing 100 µL of serum-free growth medium. Without incubating, the mixture was transferred to the microtube containing the CombiMag™ and mixed by pipetting vigorously. It was then added to the cells mixed by gentle agitation of the plate. Finally, the 6-well plate was placed upon a magnetic plate (OZ Biosciences) and incubated for 15 min. Cells were further incubated at 37 ºC in a 5% CO_2 incubator and the cell medium was changed after 6 h of transfection. 24 h after transfection cells were collected in 250 µL 1% SDS for WB.

3.6. Cell collection and quantification of protein content

Upon being collected in 250 µL 1% SDS, cells were immediately boiled at 90 ºC for 10 min, followed by a 20 sec sonication period, and stored at -20 ºC.

Quantification of the protein content of the cell lysates was made using the Pierce's bicinchoninic acid (BCA) protein assay kit (Thermo Scientific). All the procedure was performed using a 96-well plate. The standard samples needed for quantification were prepared using increasing known amounts of bovine serum albumin (BSA), as depicted in Table 3. The remaining samples were prepared by mixing 5 µL of the cell lysate to 20 µL 1% SDS.

Table 3 - Standards used in the BCA protein assay method. BSA, Bovine serum albumin solution (2 mg/ml).

Standard	BSA (µL)	10% SDS (µL)	H_2O (µL)	Protein mass (µg)
Blank	0	2,5	22,5	0
1	1	2,5	21,5	2
2	2	2,5	20,5	4
3	5	2,5	17,5	10
4	10	2,5	12,5	20
5	20	2,5	2,5	40

The Working Reagent (W.R.) was prepared by mixing the BCA reagent A with the BCA reagent B in the proportion of 50:1, and 200 µL were added to each well. The plate was incubated during 30 min at 37 ºC, after which the absorbance at 562 nm was measured using a microplate reader (Infinite M200, Tecan).

3.7. Antibodies

There were several antibodies used in western blot assays. The primary antibodies were the 22C11 (Chemicon), directed against APP N-terminus, recognizing full-length APP, and thus enabling the evaluation of the transfection levels of the APP-GFP cDNAs; anti-$G_{\alpha o}$ antibody (Upstate), for detecting Wt and CA $G_{\alpha o}$ transfection levels; both anti-actin N-terminal (Sigma) and anti-actin 2G2 (Acris antibodies) antibodies, and anti-β-tubulin (Invitrogen) antibody, for analysing the effects of $G_{\alpha o}$ and APP in cytoskeleton-related proteins. Another anti-$G_{\alpha o}$ antibody (Chemicon) was tested

but with no satisfactory results (see chapter 4.1). To evaluate the effect of $G_{\alpha o}$ and APP in STAT3 signalling two antibodies were used: the monoclonal anti-phospho-STAT3 (Millipore), directed against the phosphorylated Tyr705 residue, and the monoclonal anti-STAT3 (Cell Signalling Technology) antibodies, with both of them recognizing the alpha and beta STAT3 isoforms.

All the secondary antibodies, either recognizing mouse or rabbit antibodies, were goat antibodies labelled with horseradish peroxidase, purchased from Amersham Pharmacia. In Table 4 are represented the antibodies used, their respective dilutions and secondary antibody used.

Table 4 - Antibodies used in the Western blots, respective target proteins and their sizes, and specific dilutions used.

Target Protein/Epitope	Size (kDa)	Primary antibody	Secondary antibody
APP N-terminal	109 and 115 (endogenous); 139 and 145 (exogenous)	Monoclonal 22C11 (Chemicon); Dilution: 1:250	Horseradish Peroxidase conjugated α-Mouse IgG; Dilution: 1:5000
Alpha subunit of Go protein	39	Polyclonal Anti-$G_{\alpha o}$ (Upstate); Dilution: 1:5000	Horseradish Peroxidase conjugated α-Rabbit IgG; Dilution: 1:5000
Actin N-terminal	42	Polyclonal Anti-actin N-terminal (Sigma); Dilution: 1:1000	Horseradish Peroxidase conjugated α-Rabbit IgG Dilution: 1:500
Pan actin	42	Monoclonal Anti-actin 2G2 (Acris); Dilution: 1:2000	Horseradish Peroxidase conjugated α-Mouse IgG; Dilution: 1:5000
β-tubulin	50	Monoclonal 2-28-33 (Invitrogen) Dilution: 1:2000	Horseradish Peroxidase conjugated α-Mouse IgG Dilution: 1:5000
Phospho-Tyr705 of STAT3	76 and 84	Monoclonal Anti-phospho-STAT3 (Tyr 705) (Millipore) Dilution: 1:3000	Horseradish Peroxidase conjugated α-Rabbit IgG Dilution: 1:1000
STAT3	76 and 84	Monoclonal Anti-STAT3 (124H6) (Cell Signaling) Dilution: 1:1000	Horseradish Peroxidase conjugated α-Mouse IgG Dilution: 1:2000

For the immunocytochemistry procedures, the rabbit polyclonal anti-$G_{\alpha o}$ and anti-APP 22C11 antibodies were used, together with the mouse monoclonal anti-STAT3 (Cell Signaling). This antibody was used to analyze the influence of $G_{\alpha o}$ activation and APP phosphorylation in STAT3 signalling. Like in the WB, another anti-$G_{\alpha o}$ antibody (mouse monoclonal, Chemicon) was tested, again with no satisfactory results (Chapter

4.1). The list of the antibodies and their respective dilution and secondary antibody are present in Table 5.

Table 5 - Antibodies used in immunocytochemistry, respective target proteins specific dilutions used.

Target Protein/Epitope	Primary antibody	Secondary Antibody
APP N-terminal	Monoclonal 22C11 (Chemicon) Dilution: 1:50	Alexa Fluor® 488 Goat Anti-Mouse IgG (Life Technologies) Dilution: 1:300
Alpha subunit of Go protein	Polyclonal Anti-$G_{\alpha o}$ (Upstate) Dilution: 1:250	Alexa Fluor® 594, 488 and 350 Goat Anti-Rabbit IgG (Life Technologies) Dilution: 1:300
STAT3	Monoclonal Anti-STAT3 (124H6) (Cell Signaling) Dilution: 1:450	Texas Red®-X and Alexa Fluor® 350 goat anti-mouse IgG (Life Technologies) Dilution: 1:300

3.8. Western Blot assay

Mass-normalized cell lysates were subjected to electrophoresis on a 5-20% gradient sodium dodecylsulfate (SDS) polyacrylamide gel and then transferred to a nitrocellulose membrane. After transferring the proteins, the membranes were first soaped in 1X TBS for 10 min, and then the blockage of unspecific antibody binding sites was ensured by incubating the membrane for 1-2 h with 5% non-fat dry milk in 1X TBS-T solution. Incubation with the primary antibody was performed according to the manufacturer indications, or according to previous optimization experiments for the antibodies in use (the incubation time ranged from 2 h to O/N incubation). After 3 washes with 1X TBS-T, the membranes were incubated for 2 h with the secondary antibody. All antibodies were diluted according to the manufacturer indications (dilutions used present in table 4), normally either in 3% non-fat dry milk in 1X TBS-T solution or in 3% BSA in 1X TBS-T solution. Membranes were additionally washed 3X with TBS-T and submitted to signal development using either a home made enhanced chemiluminescence (ECL) or Luminata^{TM} Crescendo (Millipore) reagents. Both of the reagents work as a substrate to horseradish peroxidase with which the secondary antibodies are labelled, producing a chemiluminescent signal. In a dark room, the membranes were incubated for 1 min at RT with ECL or 5 min with Luminata^{TM}

Crescendo, and then an autoradiography film was placed on top of the membrane and placed inside a film cassette. After the exposure (with time varying depending on the protein being detected), the film was developed in developing solution (Sigma Aldrich), washed in water and fixed in fixing solution (Sigma Aldrich). The membrane was further washed with 1x TBS-T and deionised water before drying. The autoradiograms were scanned in a GS-800 calibrated imaging densitometer (Bio-Rad) and protein bands quantified using the Quantity One densitometry software (Bio-Rad).

3.9. Ponceau Red staining of protein bands

Ponceau Red staining is normally applied to assess successful electrotransfer of proteins to the membrane. However it can also be used as a loading control as an alternative to actin or β-tubulin, when these proteins vary with the experimental conditions. This type of staining has been described as a fast, inexpensive, and nontoxic method and it is fully reversible in a few minutes (Romero-Calvo et al., 2010).

The nitrocellulose membranes were incubated in Ponceau S solution (Sigma Aldrich) for seven min, followed by a wash with deionised water for making the protein bands clearly visible. The membrane was then scanned in a GS-800 calibrated imaging densitometer (Bio-rad). The membranes were then washed extensively with 1X TBS-T and water for completely removing the staining and thus be further used in WB assays.

3.10. Immunocytochemistry assay

Cells grown on coverslips were fixed with a 4% paraformaldehyde PBS solution for 30 min, washed 3 times with PBS and permeabilized with a 0,2% TRITON PBS solution (10 min). After another 3 washes, the cells were covered with PBS 1X/3%BSA blockage solution for 30 min. The cells were then incubated with the primary antibodies diluted in PBS 1X/3%BSA (the respective dilutions are present in Table 5) for 2 h at RT. The antibodies were removed by washing 3 times with PBS and the specific secondary antibodies were incubated for 2 h at RT (see Table 5). After 3 washes with PBS and one with deionised water, the cells were mounted with VECTASHIELD®

mounting medium, with or without DAPI (Vector Laboratories). Fluorescence microscopy was carried out using a LSM 510 Meta confocal microscope (Zeiss).

3.11. Image analysis

Every image analysis was performed using the ImageJ Fiji software. For STAT3 nuclear intensity analysis, the nuclei were selected using the LiveWire plugin and STAT3 intensity was measured. To try to optimize the comparison between different conditions without the quantifications being affected by some fluorescence/antibody labelling issues (variation in noise, signal intensity), the signal intensity of STAT3 in the nuclei of transfected cells was divided by the signal intensity in the nuclei of non-transfected cells (taken as control). Also, in every image, three measures of the background were performed and subtracted to the nuclei measure.

For colocalization analysis, the images were first processed using the DeconvolutionLab plugin for better removal of background noise and thus improving colocalization analysis (Landmann and Marbet, 2004). The colocalization analysis was conducted using the Coloc2 plugin. This plugin uses several pixel intensity spatial correlation methods to determine colocalization between two different colour channels, such as the Manders, the Costes, the Pearson or the Li methods. In the work here described, results were obtained using the Manders' method, since it is normally the most used when comparing two objects of different amounts (in this case two proteins who have different expression levels) (Manders et al., 1993). The results are presented as the percentage of colocalization of one protein with the other.

3.12. Data analysis

Data is expressed as mean ± SEM (standard error of the mean) of the different experiments. Statistical significance analysis was conducted by one way analysis of variance (ANOVA) followed by the Turkey test.

4. Results

4.1. Optimization of the transfection method and antibodies dilutions

As described in chapter 3.4, three different transfection methods were first tested in order to choose which protocol should be use throughout the experiments. Cells were seeded in 6-well plates 24h before transfection and then transfected with $G_{\alpha o}$ Wt (henceforth called just $G_{\alpha o}$) and $G_{\alpha o}$ CA for 24 hours using either jetPRIME®, TurboFect™ or CombiMag™ plus TurboFect™ transfection reagents. $G_{\alpha o}$ transfection levels were evaluated by Western Blot (WB) analysis using the polyclonal anti-$G_{\alpha o}$ antibody. As seen in Fig. 9, transfection of Go was detected in both TurboFect™ and CombiMag™ plus TurboFect™ transfected cells. While in $G_{\alpha o}$ CA there are not significant differences in the transfection levels, in $G_{\alpha o}$ there is a significant increase when using CombiMag™ plus TurboFect™. TurboFect™ was chosen as the transfection reagent for further experiments for three reasons: 1) the signal was good enough to be detected during the following experiments and 2) overexpression of a given protein could affect its normal behavior inside the cell, leading to erroneous results; 3) CombiMag™ led to an increase in cellular apoptosis, as indicated by the higher amounts of cleaved PARP (an apoptosis indicator) in those lysates (Fig. 9).

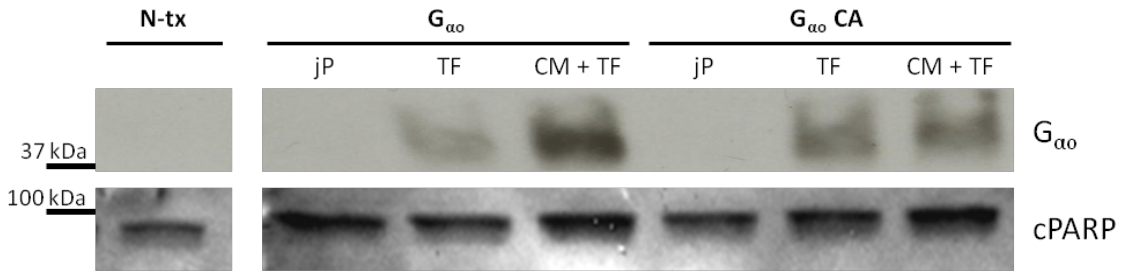

Figure 9. Immunoblot analysis of $G_{\alpha o}$ transfection in SH-SY5Y using different transfection methods. Upper blot: WB performed with the polyclonal rabbit anti-$G_{\alpha o}$ antibody to analyze transfection levels. Lower blot: WB of the same lysates performed with an anti-cleaved PARP antibody to analyze cellular apoptosis. N-tx: non-transfected cells; jP: jetPRIME® mediated transfection; TF: TurboFect™ mediated transfection; CM+TF: CombiMag™ plus TurboFect™ mediated transfection.

Two different antibodies against $G_{\alpha o}$ were acquired: a rabbit polyclonal antibody (Upstate) and a mouse monoclonal antibody (Chemicon). Both were tested in WB, with the first one working fine at a dilution of 1:5000 (recommended dilution being between 1:2000 and 1:10000), as shown in Fig. 9, while the second one never gave a signal at

the various dilutions tested (started with the recommended 1:3000 dilution and concentrate it up to 1:500). While the company sent a substitute, the new one also didn´t work, but in this case it labelled a protein with a higher molecular weight than the one supposed for $G_{\alpha o}$ (data not shown). Both antibodies were also tested in immunocytochemistry (ICC) assays, with the polyclonal antibody exhibiting a pattern that was expected from $G_{\alpha o}$, (e.g. presence at the plasma membrane), while the monoclonal antibody apparently was labelling a protein with a punctuate distribution throughout the cell (Fig. 10).

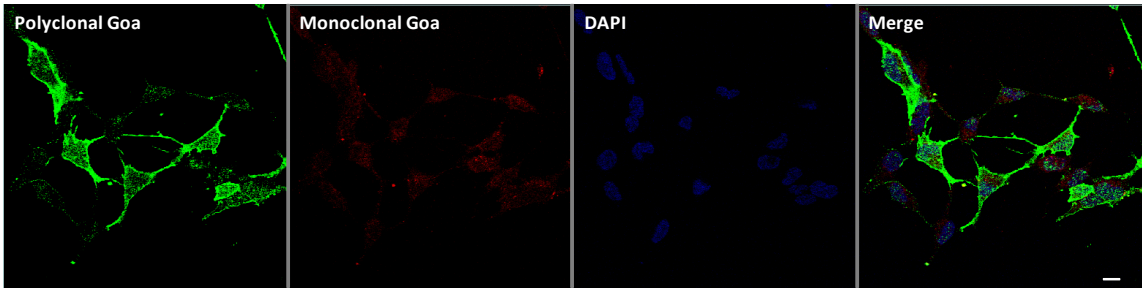

Figure 10. Immunocytochemistry of SH-SY5Y cells transfected with pcDNA3. The anti-Gαo polyclonal antibody (1:250) was marked with a secondary antibody labelled with Alexa Fluor 488 (green), while the anti-Gαo monoclonal antibody (1:250) was marked with a secondary antibody labelled with Texas Red. As expected, the polyclonal antibody marks a protein mainly present in the cell membrane, which is where $G_{\alpha o}$ is more abundant. On the contrary, the monoclonal antibody doesn't show the some kind of cellular distribution, indicating that it must be marking some protein other than $G_{\alpha o}$. Bar: 10 µm.

The antibodies against Phospho-STAT3 (P-STAT3) and STAT3 were also initially tested for WB and ICC applications. While the anti-STAT3 worked fine with the WB recommended dilution (1:1000), the anti-P-STAT3 gave a very dim signal (1:10000). Different dilutions were tested, with 1:3000 being the one that gave a more defined signal, and was thus used in the following WB experiments. For ICC applications, the recommended dilutions were effective: anti-STAT3 (1:400) and anti-P-STAT3 (1:200).

4.2. Effects of APP S655 phosphorylation and $G_{\alpha o}$ activation in APP/$G_{\alpha o}$ subcellular colocalization

As it has been previously reported and visualized in our lab, APP localizes mainly in the Golgi apparatus, with only a small fraction (less than 10%) being present

at the plasma membrane (PM) (Vieira et al., 2009; Vieira et al., 2010). On the other hand, $G_{\alpha o}$ is present across the entire cell, with predominance in the cytoplasmic face of the plasma membrane (Brabet et al., 1988; Gabrion et al., 1989). Since both proteins have been described to interact with each other, just downstream the ^{653}YTSI^{656} APP domain, the effect of S655 phosphorylation in their interaction and subcellular colocalization was tested by cotransfecting SH-SY5Y cells with both $G_{\alpha o}$ cDNA and either Wt, S655A or S655E APP-GFPs cDNAs. Undifferentiated SH-SY5Y cells were transfected during a 6 h period, after which the coverslips were recovered and ICC was performed. All the APPs are fused to GFP (green channel), while $G_{\alpha o}$ was labelled with Alexa Fluor® 594 (red channel).

First, the distributions of $G_{\alpha o}$ and $G_{\alpha o}$ CA in 6h transfected cells were analysed. Endogenous $G_{\alpha o}$, revealed by the anti-$G_{\alpha o}$ antibody, was mainly located at cells PM (where it is enriched) and in the cytoplasm (Fig. 11-A, vector transfected cells). Exogenous $G_{\alpha o}$ was highly located at the PM, slightly less at the cytoplasm (punctuated distribution) and, in cells expressing high levels of $G_{\alpha o}$, this protein was found at what appeared to be the Golgi and nearby regions (Fig. 11-B, $G_{\alpha o}$ transfected cell). In comparison with $G_{\alpha o}$, $G_{\alpha o}$ CA exhibits a similar PM/cytoplasm co-distribution, with enrichment at the PM, but leads to an increase in the number of projections (Fig. 11-C, $G_{\alpha o}$ CA transfected cells). Of note, with increasing levels of $G_{\alpha o}$ expression, its localization in the cytoplasm and Golgi increased, leading to a decrease in PM/cytoplasm localization ratio of $G_{\alpha o}$. This was even more pronounced for $G_{\alpha o}$ CA transfected cells.

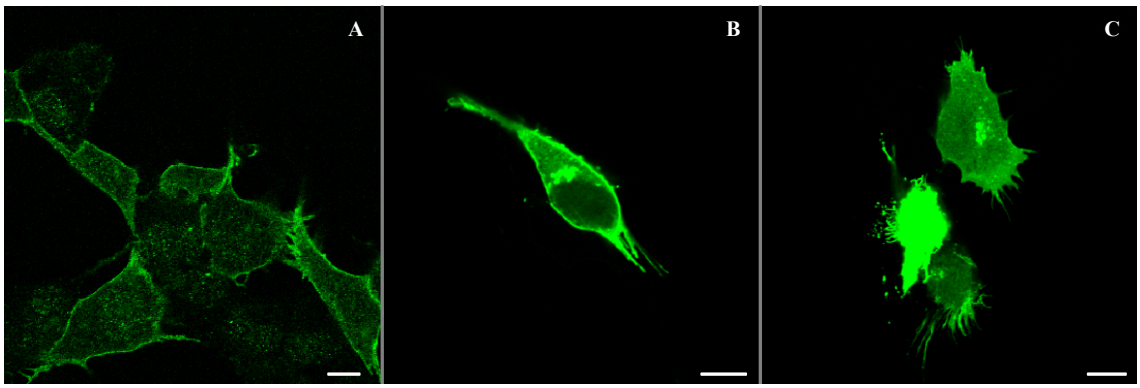

Figure 11. Subcellular localization of $G_{\alpha o}$. SH-SY5Y cells were labelled with anti-$G_{\alpha o}$ rabbit antibody. A) Cells transfected with pcDNA3; B) Cells transfected with $G_{\alpha o}$; C) Cells transfected with $G_{\alpha o}$ CA. Bar: 10 μm.

From the Wt APP-GFP/$G_{\alpha o}$ co-transfected images (Fig. 12-A) we could observe that Wt APP-GFP localizes mainly at the Golgi and ER and cytoplasmic vesicles, with the PM being only visible in some cells, and at few amounts. Again, exogenous $G_{\alpha o}$ was highly located at the PM, followed by the Golgi and the cytoplasm. The main sites of APP-GFP/$G_{\alpha o}$ colocalization were observed to be the Golgi and the PM, and, in some cells, in the PM of cells projections. While at the Golgi, APP-GFP/$G_{\alpha o}$ appear to actually co-localize, at the PM they appear to be juxtaposed (as expected). Of note, the great majority of APP-GFP vesicles does not colocalize with $G_{\alpha o}$.

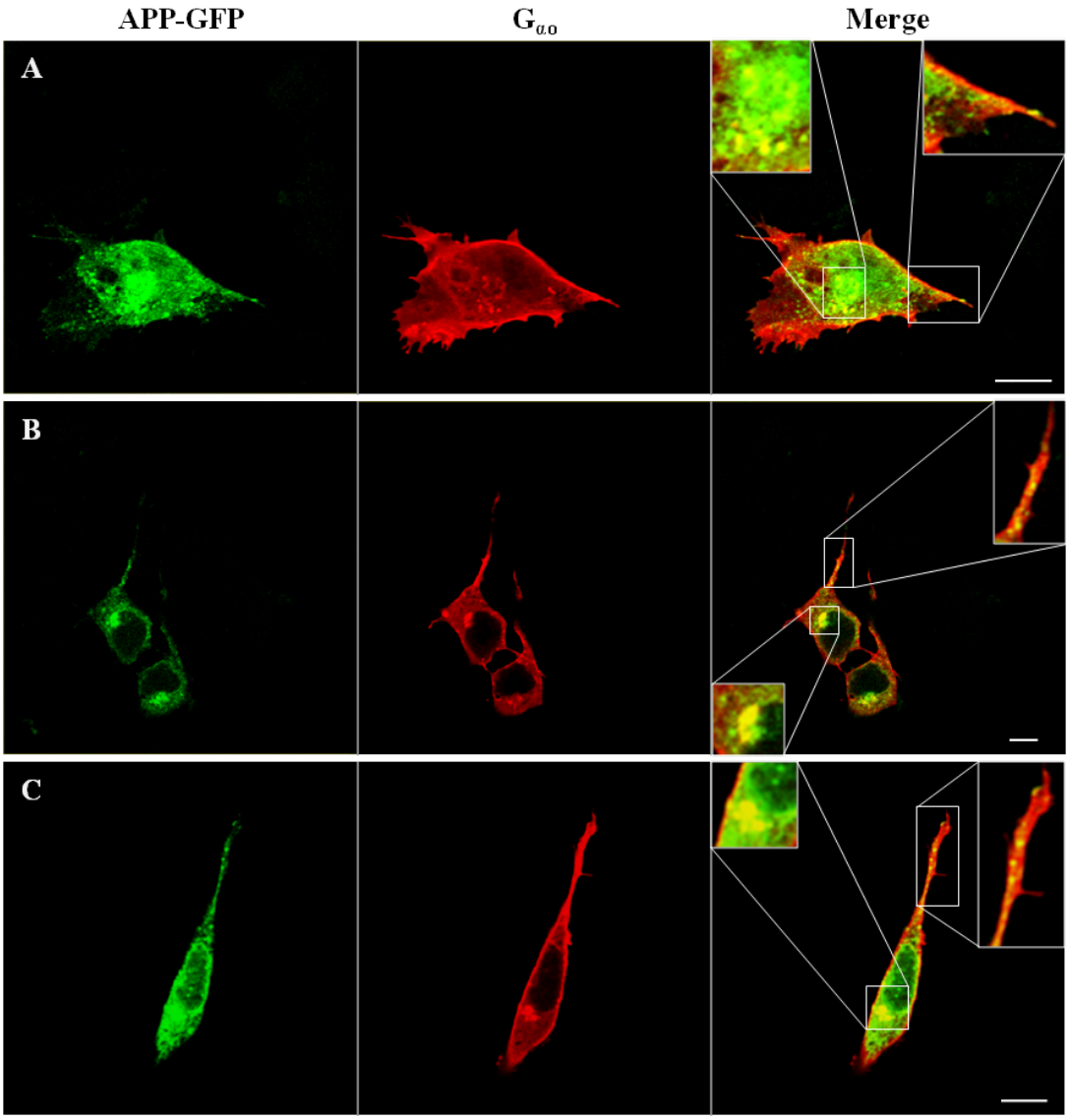

Figure 12. $G_{\alpha o}$ and APP subcellular colocalization. A) Cells cotransfected with $G_{\alpha o}$ and Wt APP-GFP; B) Cells cotransfected with $G_{\alpha o}$ and SA APP-GFP; C) Cells cotransfected with $G_{\alpha o}$ and SE APP-GFP. Bar: 10 µm

Besides this, even after the image processing prior to the colocalization analysis, the high expression of $G_{\alpha o}$ and its general distribution led to very elevated colocalization values between $G_{\alpha o}$ and APP-GFP, which may not correspond to real colocalization (Fig. 13).

Relatively to the S655 phosphomutants, the microphotographs show that, apparently, there is no significant change in APP/$G_{\alpha o}$ colocalization when $G_{\alpha o}$ is cotransfected with either S655A or S655E APP-GFPs. However, both of them increase $G_{\alpha o}$/APP-GFP colocalization when compared with the Wt APP-GFP (Fig. 12 and 13). A detailed analysis of the images reveals that the differences appeared to be due to an increased presence of APP-GFP in cellular projections. The colocalization analysis proved this to be true, especially for SA APP-GFP, where the differences were significant (Fig. 13).

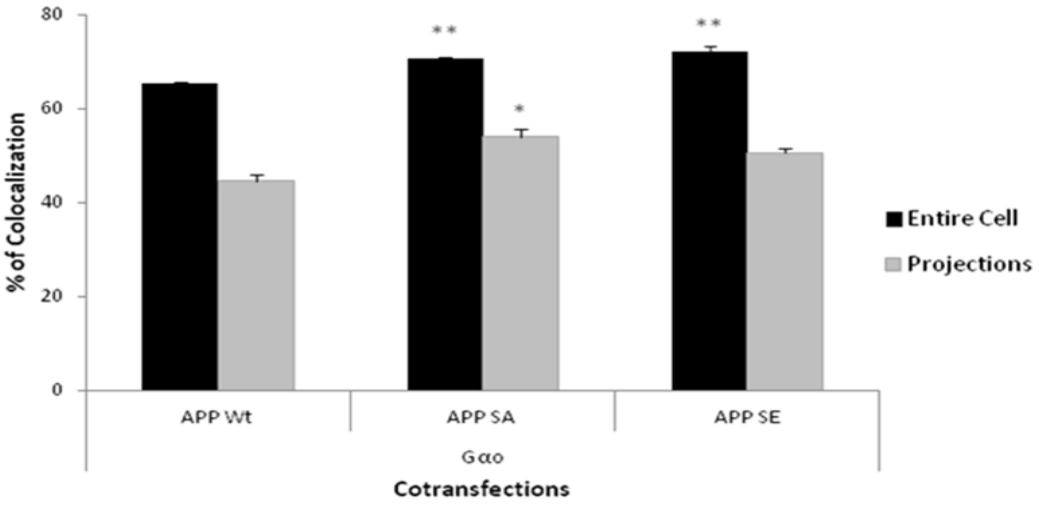

Figure 13. Colocalization of $G_{\alpha o}$ with APP-GFP in the entire cotransfected cell and in its projections. The colocalization analysis was made in cotransfected cells with $G_{\alpha o}$ and either APP Wt, APP S655A (SA) or APP S655E (SE). In each cotransfected cell the analysis was performed in the entire cell or just by selecting its projections, if they were present. Only the differences between $G_{\alpha o}$:APP Wt and either $G_{\alpha o}$:APP SA or $G_{\alpha o}$:APP SE were significant for the entire cell, and between $G_{\alpha o}$:APP Wt and $G_{\alpha o}$:APP SA for the cell projections. *$p<0.05$; **$p<0.01$; ***$p<0.001$. n=3, with each group containing 10 cells.

The effect of $G_{\alpha o}$ activation in $G_{\alpha o}$/APP-GFP colocalization was also studied. This time, the different APP-GFPs constructs were cotransfected with a constitutively active (CA) $G_{\alpha o}$ cDNA for 6 h. The same analysis procedure was performed as for APP/$G_{\alpha o}$ cotransfected cells, and the same problems arose, with $G_{\alpha o}$ CA high expression levels hindering the colocalization analysis. Nevertheless, comparative to APP-GFP/$G_{\alpha o}$ distribution, $G_{\alpha o}$ activation slightly increased $G_{\alpha o}$/APP-GFP colocalization for both Wt

and SE APP-GFPs (compare Fig. 13 with Fig. 15). A more detailed analysis reveals that $G_{\alpha o}$ CA exhibits a similar PM/cytoplasm co-distribution that $G_{\alpha o}$ but, as it induces morphological alterations that result in higher PM surface area, it has a higher pool at the PM available to colocalize with APP-GFP, potentially explaining its higher colocalization with the Wt and SE APP-GFP proteins. All APP-GFP proteins colocalize with $G_{\alpha o}$ CA in the same subcellular structures as for $G_{\alpha o}$: Golgi, PM and cellular projections (Fig. 14).

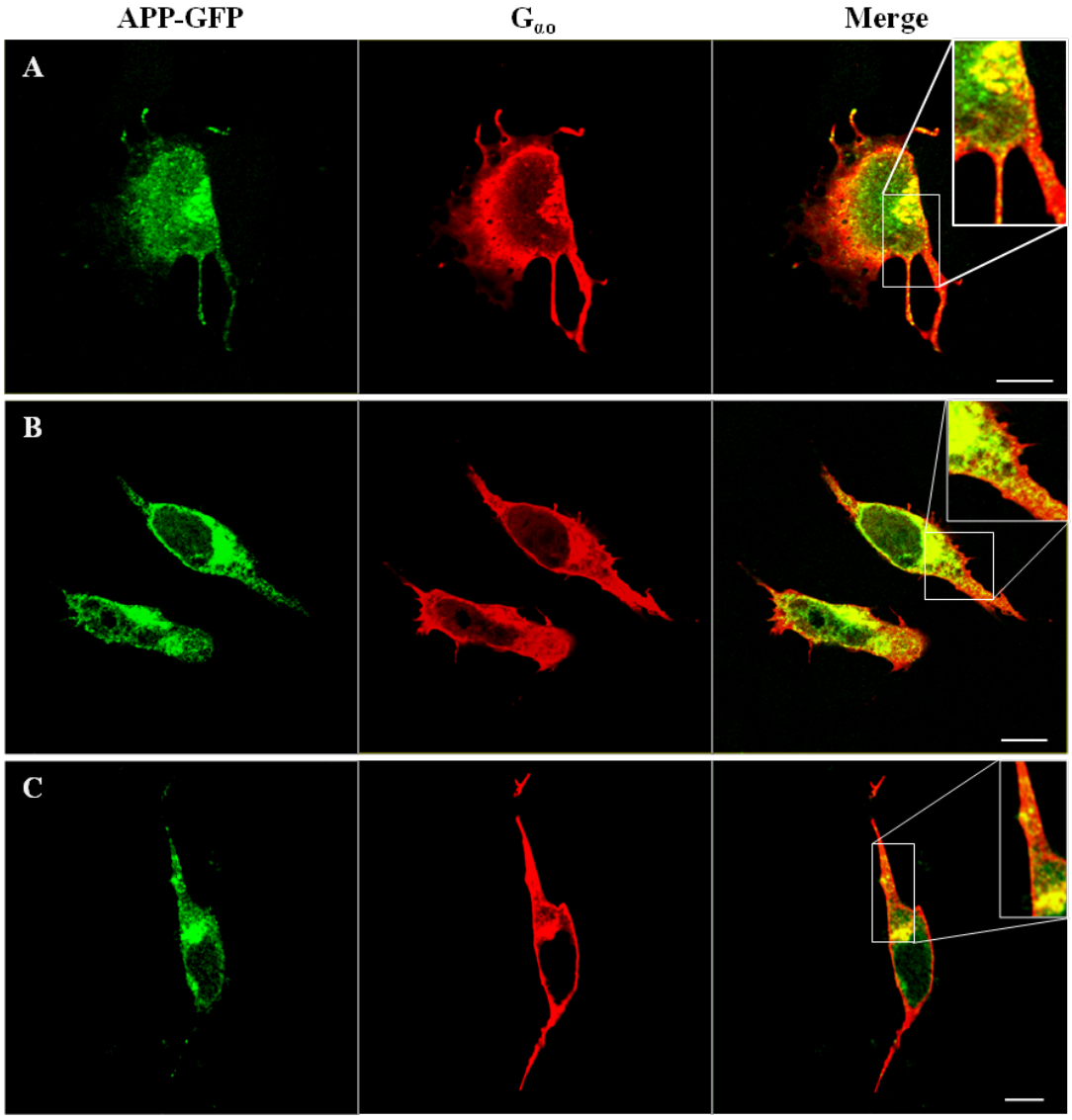

Figure 14. $G_{\alpha o}$ CA and APP subcellular colocalization. A) Cells cotransfected with $G_{\alpha o}$ CA and Wt APP-GFP; B) Cells cotransfected with $G_{\alpha o}$ CA and SA APP-GFP; C) Cells cotransfected with $G_{\alpha o}$ CA and SE APP-GFP. Bar: 10 µm

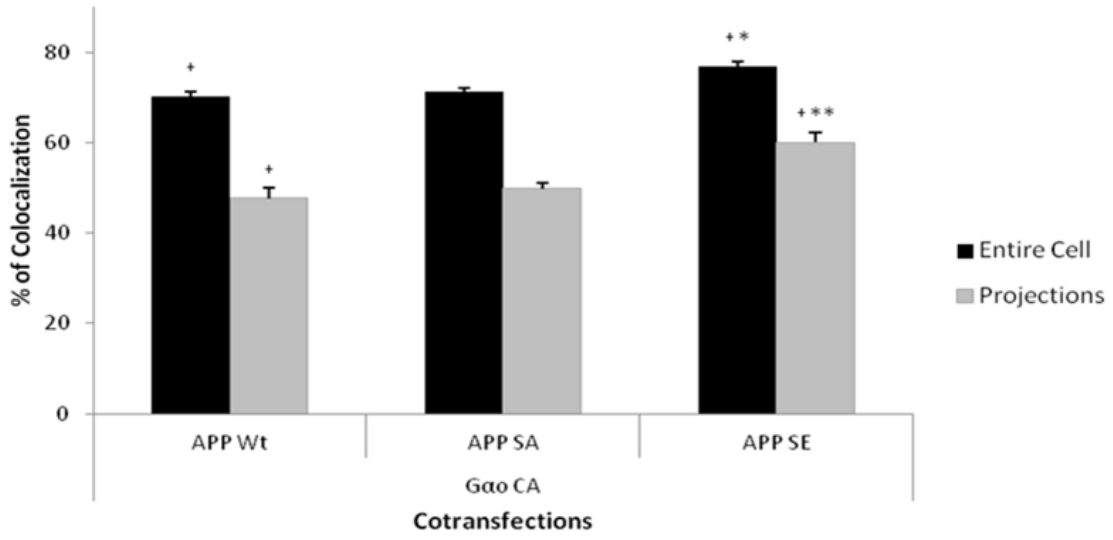

Figure 15. Colocalization of $G_{\alpha o}$ CA with APP-GFP in the entire cell and in its projections. The colocalization analysis was made in cotransfected cells with $G_{\alpha o}$ CA and either APP Wt, APP SA or APP SE. In each cotransfected cell the analysis was performed in the entire cell or just by selecting its projections, if they were present. Each cotransfection was compared with either its $G_{\alpha o}$ counterpart: $^{+}p<0.05$; $^{++}p<0.01$; $^{+++}p<0.001$; or between APP-GFP constructs: *p<0.05; **p<0.01; ***p<0.001. n=3, with each group containing 10 cells.

Since high expression of transfected $G_{\alpha o}$ made colocalization analysis difficult, we decided to do a qualitative $G_{\alpha o}$ and APP colocalization analysis in non-transfected cells. Immunocytochemistry was performed in SH-SY5Y cells using anti-$G_{\alpha o}$ and 22C11 (APP) antibodies. Results show that, indeed, potential colocalization sites occur at the PM and in what appears to be the Golgi area (Fig. 16).

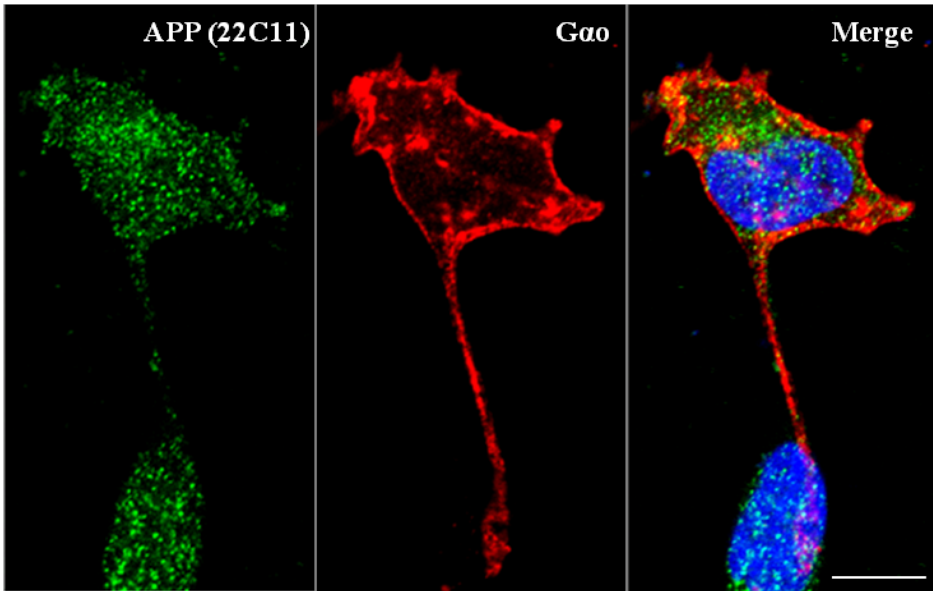

Figure 16. Subcellular localization of $G_{\alpha o}$ and APP in non-transfected SH-SY5Y. $G_{\alpha o}$ was labelled with anti-$G_{\alpha o}$ and APP was labelled with 22C11 antibody. Bar: 10 µm

4.3. $G_{\alpha o}$/APP-induced alterations in cellular morphology

Both G_o protein and APP have been implied (described?) in neuritogenesis and since they interact with each other, APP could be promoting neuritogenesis through Go activation. To study this hypothesis, and since some morphological changes were already seen in the microphotographs, the number of projections arising from cells was counted, in the APP-GFP/$G_{\alpha o}$ and $G_{\alpha o}$ CA co-expressing cells. As control, the projections in non-transfected cells, pcDNA3, $G_{\alpha o}$ and $G_{\alpha o}$ CA transfected cells were also counted.

When $G_{\alpha o}$ was singly transfected, its overexpression significantly increased the number of projections when compared to non-transfected cells (~6 times). Moreover, all cotransfections were able to increase the number of projections in comparison with non-transfected cells. In opposition, only $G_{\alpha o}$ and its cotransfection with Wt APP-GFP increased the number of projections over the pcDN3 transfection. Interestingly, $G_{\alpha o}$ cotransfection with SA and SE APP-GFPs lead to a slight decrease in the number of projections when compared with $G_{\alpha o}$ alone (see Fig. 12 and 17). Interestingly, while not affecting the number of projections, SA and mainly SE APP-GFP seemed to lead to an increase in the projections length (Fig.12 and 14; results further ahead).

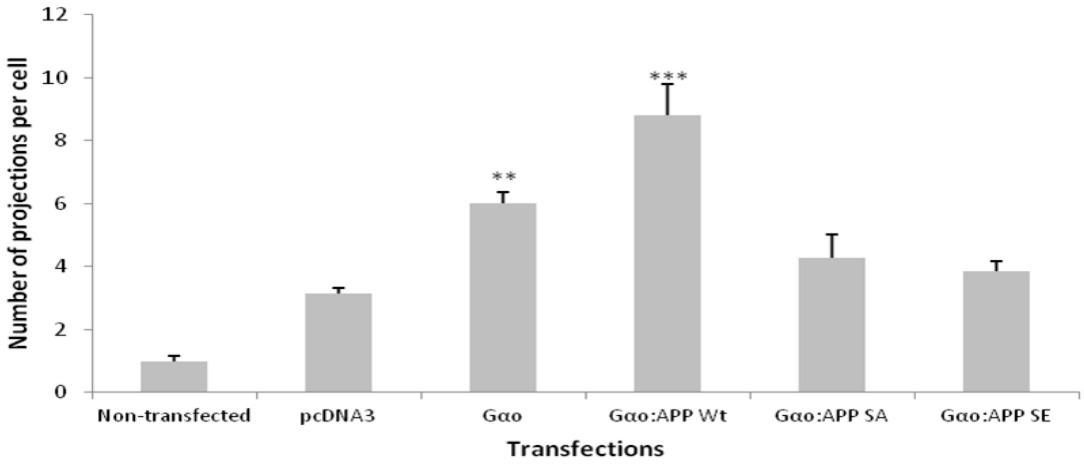

Figure 17. Number of projections per cell in SH-SY5Y cells. The number of projections was counted in non-transfected cells, pcDNA3 and $G_{\alpha o}$-only transfected cells, and $G_{\alpha o}$ cotransfection with either Wt, SA or SE APP-GFP. Each transfection was compared to pcDNA3 transfected cells. *p<0.05; **p<0.01; ***p<0.001. n=3, with each group containing 10 cells.

Regarding $G_{\alpha o}$ CA, and as already observed, its overexpression increased the number of projections when compared to $G_{\alpha o}$ (Fig. 11 and 18). However, when

compared to $G_{\alpha o}$, $G_{\alpha o}$ CA only significantly increased the number of projections in the SA APP-GFP cotransfections, while in the other cotransfections its effect was no different of $G_{\alpha o}$ (Fig. 14 and 18). Interestingly, the number of projections in $G_{\alpha o}$ CA and $G_{\alpha o}$:Wt APP-GFP expressing cells is roughly the same, as for SA APP-GFP, while SE APP-GFP decrease their number by half (Fig. 17 and 18).

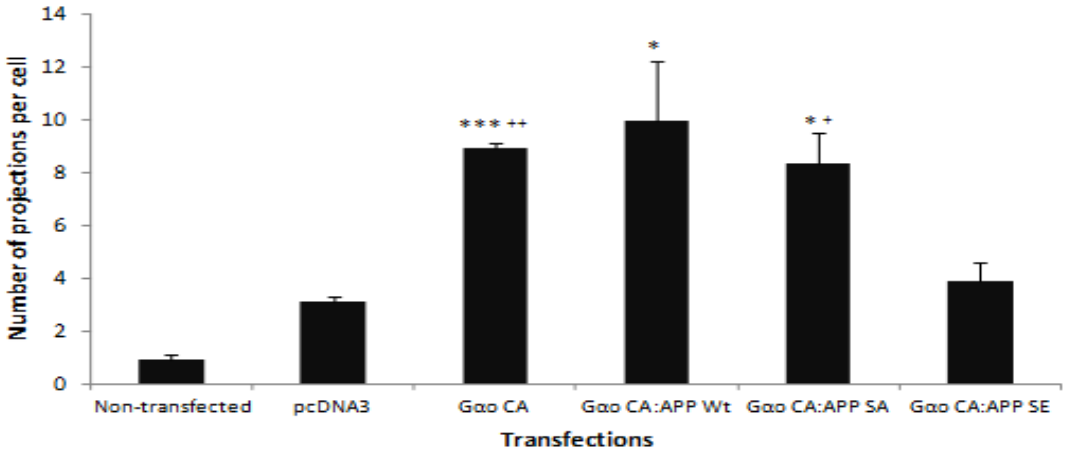

Figure 18. Number of projections per cell in SH-SY5Y cells. The number of projections was counted in non-transfected cells, pcDNA3, $G_{\alpha o}$ CA-only transfected cells and in cells cotransfected with $G_{\alpha o}$ CA and with either Wt, SA or SE APP-GFP. Each transfection was compared with either pcDNA3 transfected cells: *p<0.05; **p<0.01; ***p<0.001; or with its $G_{\alpha o}$ counterpart: $^{+}$p<0.05; $^{++}$p<0.01; $^{+++}$p<0.001. n=3, with each group containing 10 cells.

As mentioned earlier, while cotransfection with APP-GFP phosphomutants did not change the number of projections, it apparently led to an increased number of cells with longer projections (Fig. 12). Hence, we further scored the number of cells with projections longer than the cell body, typically named pre-neurites (PreN) (Fig. 19).

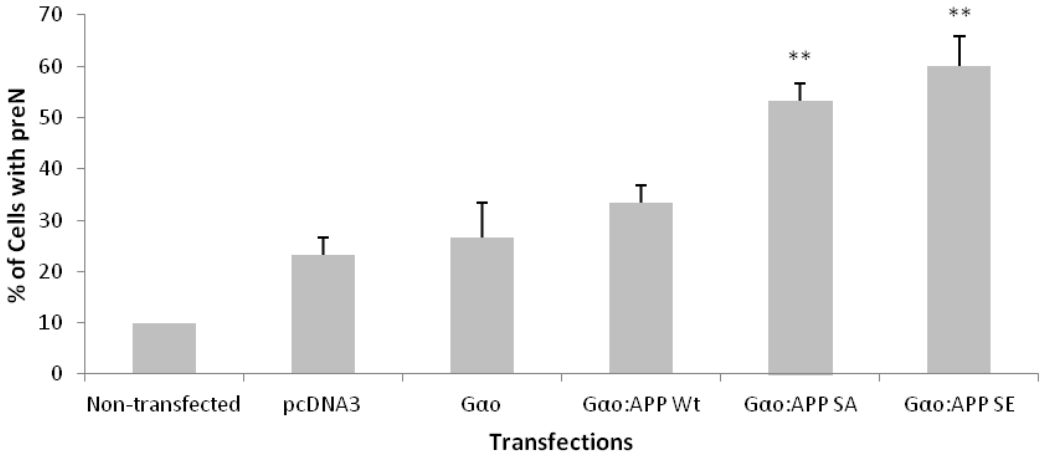

Figure 19. Percentage of cells with Pre-Neurites in SH-SY5Y non-transfected and transfected cells. The number of cells with pre-neurites was counted in non-transfected cells, pcDNA3 and $G_{\alpha o}$-only transfected cells, and $G_{\alpha o}$ cotransfection with either Wt, SA or SE APP-GFP. Each transfection was compared to pcDNA3 transfected cells. *p<0.05; **p<0.01; ***p<0.001. n=3, with each group containing 10 cells.

As seen in Fig. 19, indeed cotransfection of $G_{\alpha o}$ with SA and SE APP-GFPs increased the length of projections, without increasing their number. Wt APP-GFP, in its turn, is able to increase cellular projections but it does not significantly alter their length. $G_{\alpha o}$ is not able to increase the number of cells with pre-neurites.

When transfected with $G_{\alpha o}$ CA, the number of cells with preN slightly increased over $G_{\alpha o}$ data, and the same occurred for the Wt APP-GFP/$G_{\alpha o}$ CA, when compared to Wt APP-GFP/$G_{\alpha o}$ cotransfected cells. However, probably due to the small size of the sample, these changes were not significant. In opposition to the Wt data, the number of cells bearing preN cotransfected with $G_{\alpha o}$ CA and SA or SE APP-GFP did not significantly change when compared to SA or SE APP-GFP/$G_{\alpha o}$ cotransfected cells (Fig. 20).

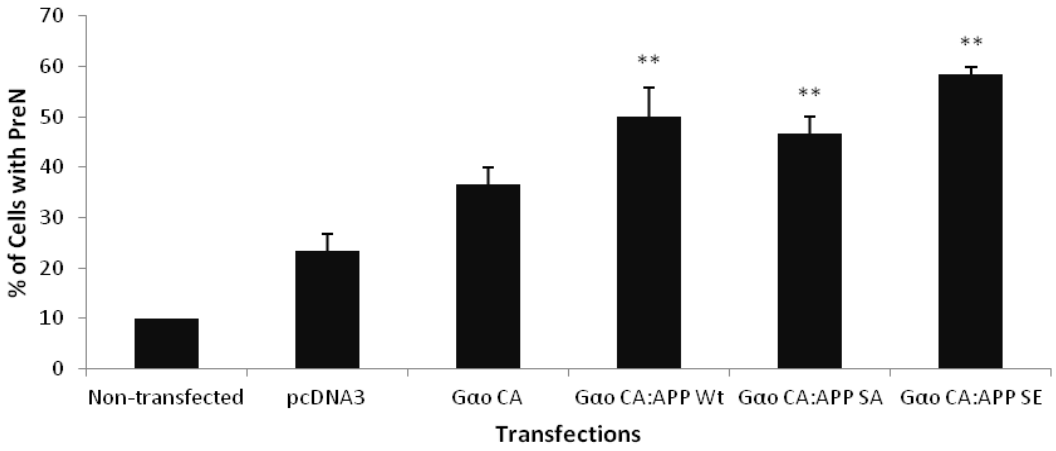

Figure 20. Percentage of cells with Pre-Neurites in SH-SY5Y non-transfected and transfected cells. The number of cells with pre-neurites was counted in non-transfected cells, $G_{\alpha o}$ CA-only transfected cells and $G_{\alpha o}$ CA cotransfection with either Wt, SA or SE APP-GFP. Each $G_{\alpha o}$ CA transfection was compared with its $G_{\alpha o}$ counterpart. $^{+}p<0.05$; $^{++}p<0.01$; $^{+++}p<0.001$. n=3, with each group containing 10 cells.

4.4. Analysis of cytoskeleton-related protein profiles

Since $G_{\alpha o}$ overexpression induced morphological changes, possible changes in cytoskeleton proteins, namely actin and tubulin, were evaluated. Cells were collected after 6 h of transfection and WB assay was performed (Fig. 21).

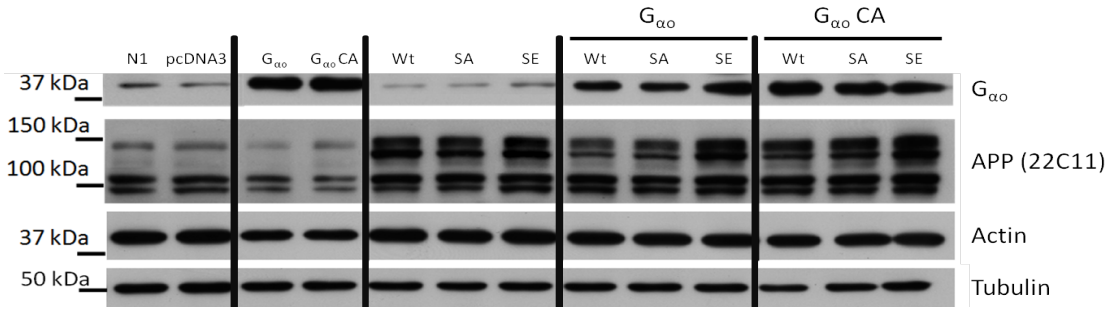

Figure 21. Immunoblot analysis of actin and tubulin levels in SH-SY5Y transfected cells. Besides WB of actin and tubulin, $G_{\alpha o}$ and APP were also visualized to confirm that they were successfully transfected and cotransfected. N1: pEGFP-N1 vector; pcDNA3: pcDNA3 vector.

Actin and Tubulin protein bands were quantified by densitometry, corrected to Ponceau relative levels, and plotted graphically (Fig. 22).

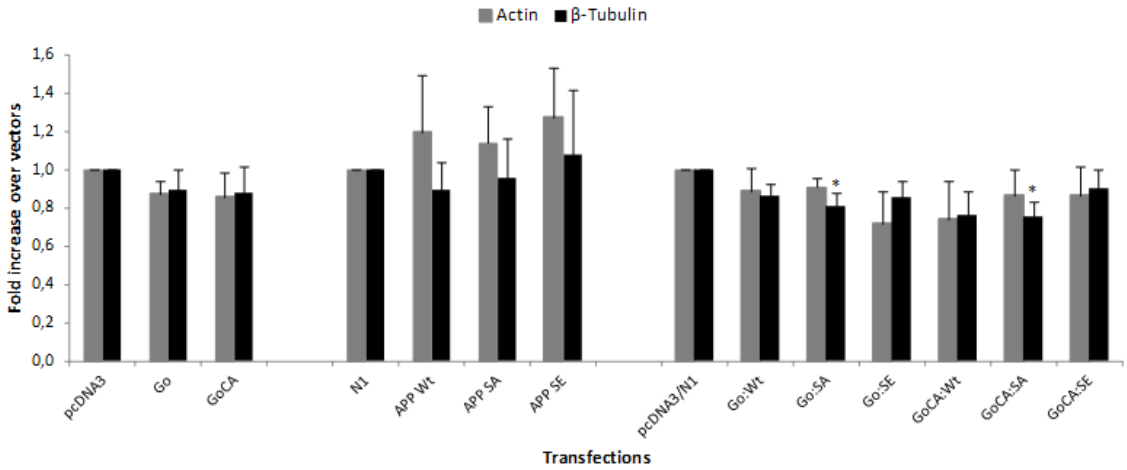

Figure 22. Evaluation of Actin and β-tubulin expression levels. Expression of actin and β-tubulin was evaluated after 6 h of transfection with different cDNAs. Each value was corrected using Ponceau Red staining as control, and plotted against the levels of its corresponding vector, taken as 1. *p<0.05; **p<0.01; ***p<0.001. n=5

The results indicate that there is a high degree of variation in actin levels when transfected with either $G_{\alpha o}$ or APP-GFP cDNAs. There seems to exist a tendency for either $G_{\alpha o}$ or $G_{\alpha o}$ CA to decrease actin levels, while all forms of APP tend to increase it. When both proteins are cotransfected, there is also a tendency for actin to decrease. However, due to the high actin variability seen, these differences are not statistically significant. In general, tubulin levels tend to slightly decrease with $G_{\alpha o}$ or APP-GFPs transfections, but this is more accentuated for $G_{\alpha o}$/APP-GFP cotransfections, and especially significant for $G_{\alpha o}$/$G_{\alpha o}$ CA co-transfection with SA APP-GFP (Fig. 22).

4.5. Effects of APP in $G_{\alpha o}$-induced STAT3 activation

4.5.1. Nuclear STAT3 changes in response to $G_{\alpha o}$ overexpression

One of the pathways already described by which $G_{\alpha o}$ leads to neurite growth is the STAT3 pathway (He et al., 2005). To test the effect of APP in $G_{\alpha o}$-induced STAT3 activation, we first tested the effect of $G_{\alpha o}$ and $G_{\alpha o}$ CA in STAT3 signalling in SH-SY5Y cells, in order to establish control conditions. Accordingly, we first intended to perform a double immunocytochemistry using the anti-$G_{\alpha o}$ mouse antibody to mark the transfected cells and the rabbit anti-P-STAT3 antibody to visualize STAT3 phosphorylation levels, and thus STAT3 activation. However, as mentioned above the anti-$G_{\alpha o}$ mouse antibody never functioned (see chapter 4.1). Hence, for visualization of $G_{\alpha o}$ transfected cells we had to use the rabbit antibody, making it impossible to use at the same time the anti-P-STAT3 antibody. Since phosphorylation of STAT3 results in its dimerization and subsequent translocation to the nucleus (Sehgal, 2008), we used the anti-STAT3 antibody instead and tried to indirectly measure STAT3 activation by measuring STAT3 nuclear intensity in transfected cells.

In our first experiment, SH-SY5Y cells were transfected with pcDNA3 vector, $G_{\alpha o}$ and $G_{\alpha o}$ CA cDNAs, and cells fixed upon 6 and 24 h of transfection. Double ICC was performed using polyclonal anti-$G_{\alpha o}$ and monoclonal anti-STAT3 antibodies, while the nucleus was labelled with DAPI (Fig. 23).

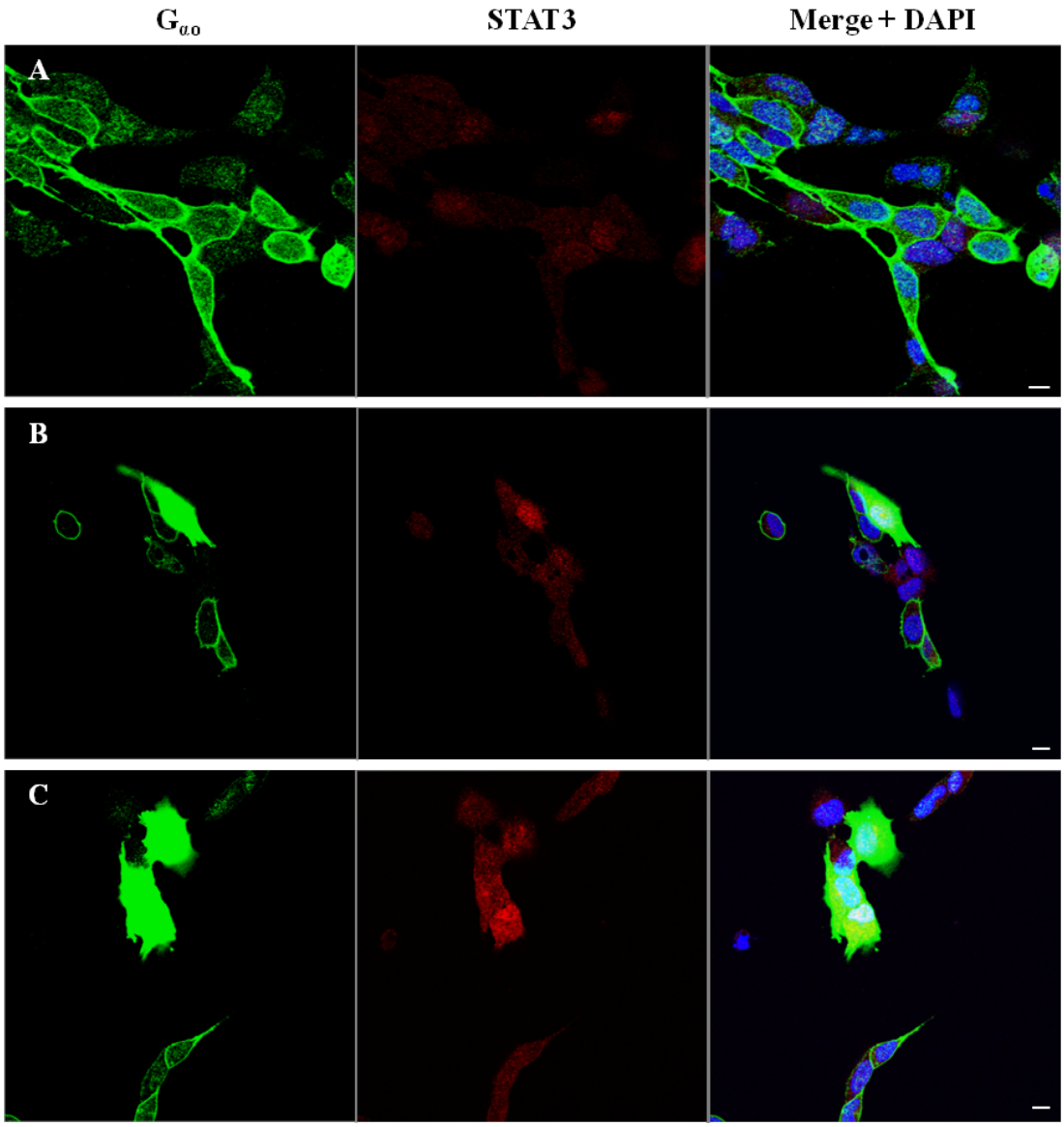

Figure 23. Nuclear STAT3 levels in $G_{\alpha o}$ expressing cells. A) Cells transfected with pcDNA3; B) Cells transfected with $G_{\alpha o}$; C) Cells transfected with $G_{\alpha o}$ CA. ICC was performed after 6 h of transfection. Bar: 10 μm.

In pcDNA3 transfected cells we could observe medium and low endogenous $G_{\alpha o}$ levels, while in $G_{\alpha o}$ or $G_{\alpha o}$ CA transfected cells we also observe high levels of $G_{\alpha o}$ expression. This led us to divide the cells into three categories: low, medium and high/transfected $G_{\alpha o}$ cells. Nuclear STAT3 (nSTAT3) mean intensity was measured in all these cell categories and compared between them (Fig. 24-A). Also, for a better comparison between different conditions, the mean intensities of nSTAT3 in cells exhibiting medium and high/transfected $G_{\alpha o}$/$G_{\alpha o}$ CA levels were further compared to mean intensities of neighbour cells with low $G_{\alpha o}$ levels, taken as 1. This allowed minimizing the influence of fluorescence differences between different transfection

conditions (Fig. 24-B). All images were analysed using Fiji, with DAPI labelling being used to delimit the nuclear area.

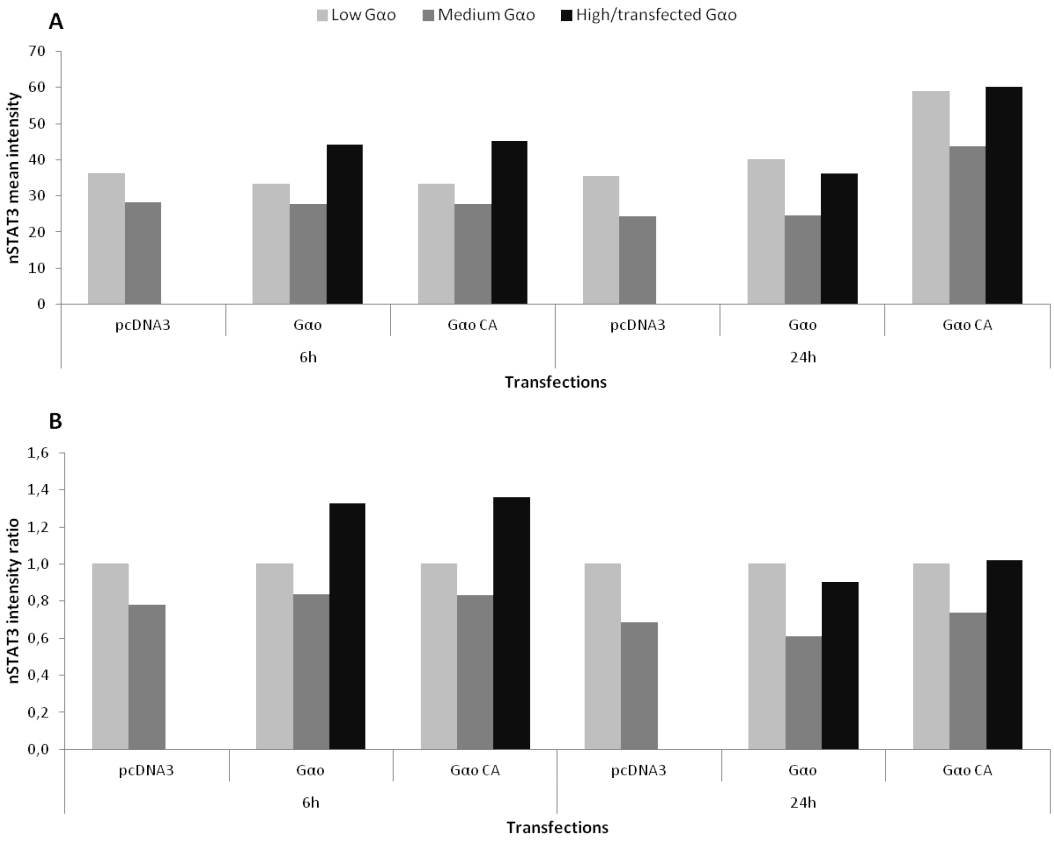

Figure 24. Nuclear STAT3 mean intensity. A) Raw nSTAT3 mean intensity in pcDNA3, $G_{\alpha o}$ and $G_{\alpha o}$ CA transfected cells. B) Comparison between nSTAT3 mean intensity of cells with medium/high $G_{\alpha o}$ expression and the nSTAT3 intensity of cells expressing low $G_{\alpha o}$ levels (taken as 1). n=1 where 30 cells were evaluated

The results show that cells that appear to have been transfected with either $G_{\alpha o}$ or $G_{\alpha o}$ CA have higher nSTAT3 intensity than non-transfected cells at 6 h. However, at 24 h, these levels have decreased and equalled the ones of cells expressing low levels of $G_{\alpha o}$. Interestingly, cells that appear to be expressing medium levels of endogenous $G_{\alpha o}$ ('medium $G_{\alpha o}$ cells') have lower nuclear STAT3 intensity, with this being clearly visible in the microphotographs (Fig. 23).

The time point of 6 h of transfection was chosen from the results of a previous WB assay where several $G_{\alpha o}$ transfection times were tested for STAT3 activation. As seen in Fig. 25, P-STAT3 levels were higher (when compared to pcDNA3 vector) at 6h, and this time point was therefore confirmed to be the appropriated to study the effects of APP on $G_{\alpha o}$-induced STAT3 activation (Fig. 25).

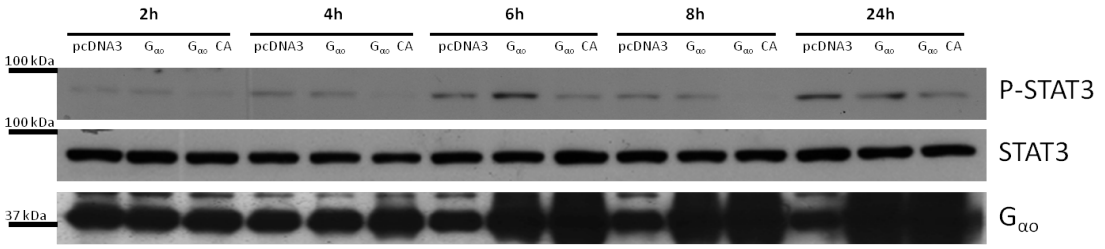

Figure 25. Immunoblot analysis of Phospho-STAT3 (upper blot) and STAT3 (medium blot) levels at several hours of transfection with pcDNA3, $G_{\alpha o}$ or $G_{\alpha o}$ CA cDNAs ($G_{\alpha o}$ expression in lower blot).

Further and of some importance, while in the WB we could only detect the STAT3 activation phase for $G_{\alpha o}$ and at 6h, for the other time points on, and for all the $G_{\alpha o}$ CA lysates, we could only detect a downregulation phase following activation (Fig 25). This inhibiting phase correlated very well with the equal and lower levels of nSTAT3 of cells expressing high and medium amounts of $G_{\alpha o}$ at 24h (Fig. 24, 24h). Hence, higher nSTAT3 targeting above non-transfected cells levels is a good method to visualize immediate $G_{\alpha o}$-induced STAT3 activation, while lower nSTAT3 targeting, below non-transfected cells levels appears to correlate with a down regulation phase following $G_{\alpha o}$-induced STAT3 activation (Fig. 24-B). This is corroborated by findings from our group where this retroinhibition mechanism is accompanied by severe decrease in $G_{\alpha o}$ levels, as it may occur in the medium-expressing cells.

4.5.2. APP phosphorylation influences $G_{\alpha o}$-induced STAT3 activation

The next step was to see if APP phosphorylation influenced STAT3 activation induced by $G_{\alpha o}$ overexpression. Undifferentiated SH-SY5Y cells were cotransfected for 6 h, after which cells were fixed and ICC was performed: cells were labelled with green fluorescing APP-GFP, red fluorescing $G_{\alpha o}$ (labelled with Alexa Fluor® 594) and blue fluorescing STAT3 (labelled with Alexa Fluor® 350) (Fig 26 and 27). Of note, in this ICC the mounting media containing DAPI could not be used. Thus, to evaluate the nuclear STAT3 levels in cotransfected cells, a qualitatively analysis was performed in two ways: 1) by visually comparing nuclear STAT3 levels in cotransfected cells and in the surrounding non-transfected cells, and 2) comparing the distribution of STAT3 levels between the nuclei (depicted by APP-GFP labelling) and the cytoplasm of cotransfected cells. The nuclear STAT3 levels were so divided in three categories: lower, equal and higher nSTAT3 (Fig. 28).

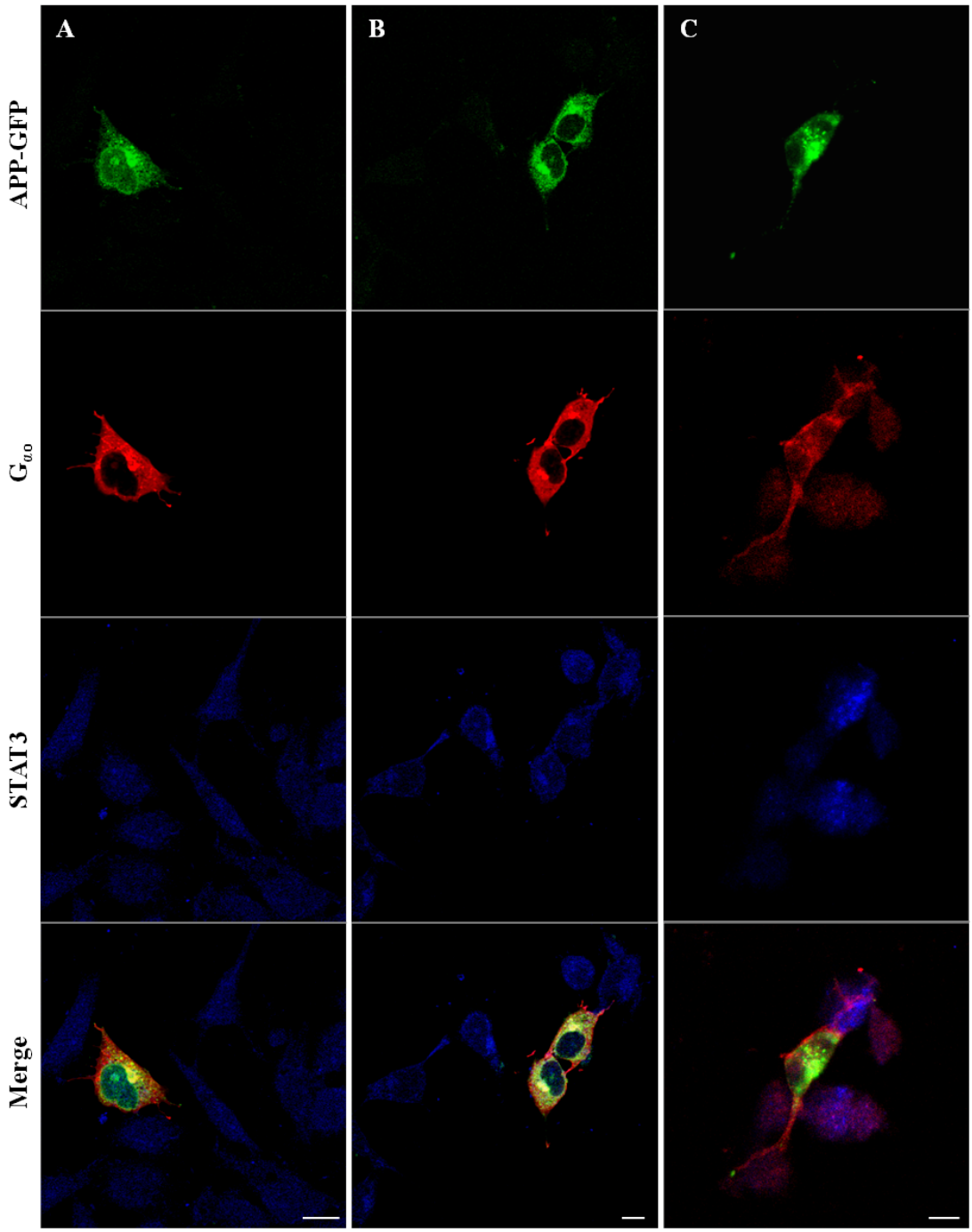

Figure 26. Analysis of nuclear STAT3 levels in APP-GFP and $G_{\alpha o}$ transfected cells. A) Cells cotransfected with $G_{\alpha o}$ and Wt APP-GFP; B) Cells cotransfected with $G_{\alpha o}$ and SA APP-GFP; C) Cells cotransfected with $G_{\alpha o}$ and SE APP-GFP. Bar: 10 µm

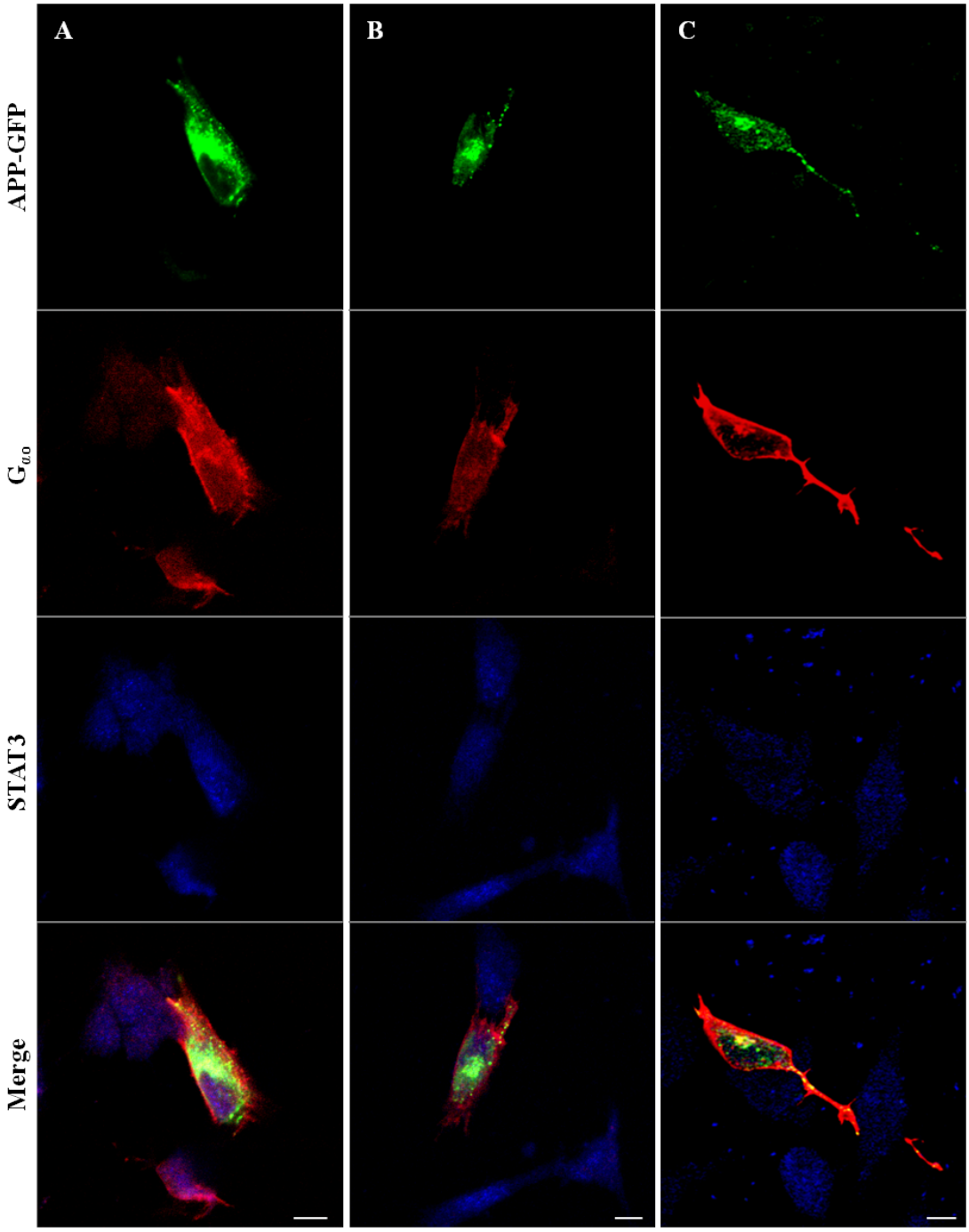

Figure 27. Analysis of nuclear STAT3 levels in APP-GFP and $G_{\alpha o}$ CA transfected cells. A) Cells cotransfected with $G_{\alpha o}$ CA and Wt APP-GFP; B) Cells cotransfected with $G_{\alpha o}$ CA and SA APP-GFP; C) Cells cotransfected with $G_{\alpha o}$ CA and SE APP-GFP. Bar: 10 μm

The results seem to indicate that cotransfection with APP-GFPs constructs leads to a decrease in $G_{\alpha o}$-induced STAT3 activation (or increase in a retro-inhibition mechanism upon STAT3 activation), since there is a higher cell percentage with equal or lower levels of nSTAT3 than higher levels. While not being statistically significant,

this phenomenon appears to be more pronounced when $G_{\alpha o}$ is cotransfected with SE APP-GFP, and less for $G_{\alpha o}$:Wt APP-GFP cotransfection (higher number of cells with increased nSTAT3) (Fig. 28-A).

As seen in Figure 28-B, cotransfections with $G_{\alpha o}$ CA led to a shift of the nSTAT3 intensity profiles to the right (more activation) for the Wt and SA APP-GFP, while leading to a shift for the left for the SE APP-GFP mutant (more inactivation).

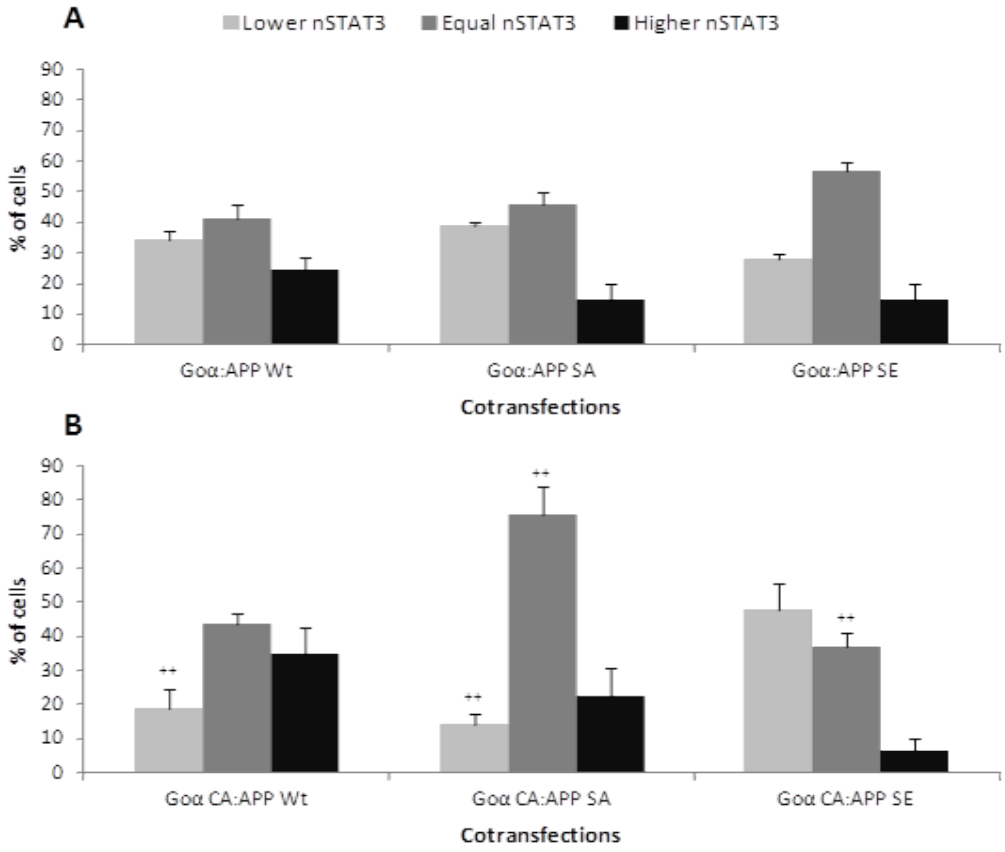

Figure 28. Qualitative analysis of nuclear STAT3 levels in APP/$G_{\alpha o}$ cotransfected cells by comparison of nuclear STAT intensity of cotransfected versus neighbour non-transfected cells. A) nSTAT3 levels in cotransfected cells with $G_{\alpha o}$ and either Wt, SA or SE APP-GFP. B) nSTAT3 levels in cotransfected cells with $G_{\alpha o}$ CA and either Wt, SA or SE APP-GFP. Each $G_{\alpha o}$ CA transfection was compared with its $G_{\alpha o}$ counterpart. $^{+}p<0.05$; $^{++}p<0.01$; $^{+++}p<0.001$. n=3, with each group containing 10 cells.

The problem with this analysis is that being qualitative, it makes comparisons with the previous experiment difficult to perform, so one has to be careful when drawing conclusions from these results. In order to try to overcome this problem, a quantitative analysis was also performed. However, as it was previously mentioned, without DAPI to indentify the nuclei we had to use the APP-GFP labelling to delimit the nuclei in transfected cells, while on non-transfected cells the centre of the cell body was manually selected. Fortunately, in most cases it was easy to see the location of the nucleus since there was a significant increase or decrease in non-transfected nSTAT3.

The mean intensity was first measured in transfected cells and compared between conditions (Fig. 29). The results show a pattern similar to the qualitative analysis, with APP phosphomutants generally showing lower nSTAT3 levels when compared with Wt APP-GFP, in $G_{\alpha o}$ cotransfections, and with $G_{\alpha o}$ CA being able to increase the levels of nSTAT3 when cotransfected with SA APP-GFP, while decreasing nSTAT3 levels for the SE mutant.

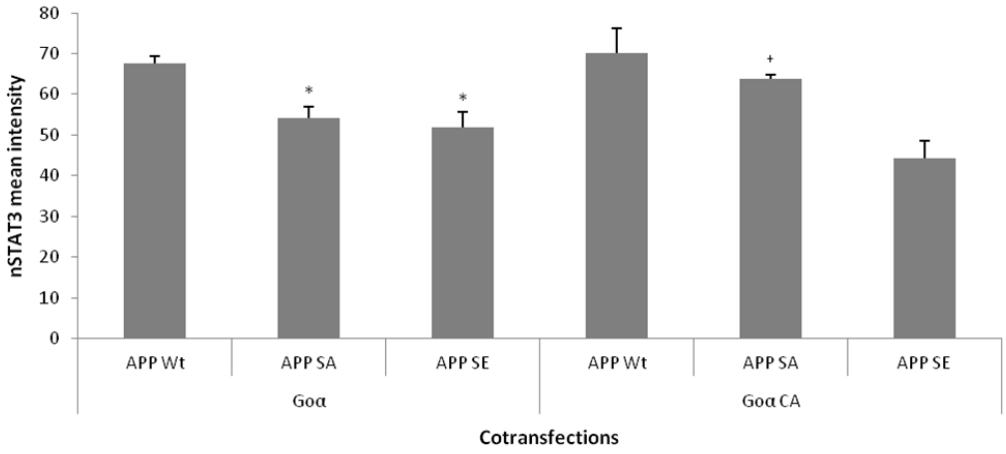

Figure 29. Quantitative analysis of Nuclear STAT3 levels in $G_{\alpha o}$/APP-GFP cotransfected cells. nSTAT3 mean intensity in cotransfected cells. *: comparison performed in $G_{\alpha o}$ cotransfected cells between Wt APP-GFP and SA or SE APP-GFP; +: comparison between $G_{\alpha o}$ CA and $G_{\alpha o}$ cotransfected cells. *p<0.05; **p<0.01; ***p<0.001. n=3, with each group containing 10 cells.

5. Discussion

With this work we intended to study cellular interactions between APP and $G_{\alpha o}$ proteins, namely their subcellular colocalization, their capability of inducing neurite outgrowth and activating the STAT3 pathway, together with the effect of APP phosphorylation and $G_{\alpha o}$ activation in those processes.

We first determined that the TurboFect^{TM} transfection reagent was the most suitable for our experiments. While jetPRIME didn't induce any significant transfection, both TurboFect^{TM} and the combination of TurboFect^{TM} with CombiMag^{TM} were able to induce transfection of both $G_{\alpha o}$ and $G_{\alpha o}$ CA cDNAs. TurboFect^{TM} was chosen over CombiMag^{TM} plus TurboFect^{TM} because the latter, although inducing a higher transfection rate, also led to increased apoptosis, measured via the amount of cleaved PARP (Fig. 9). Also, in previous work conducted in the lab, TurboFect^{TM} was used to transfect APP-GFP cDNAs in SH-SY5Y cells with satisfactory results (Rocha, 2011).

Following, we observed the SH-SY5Y subcellular sites of $G_{\alpha o}$ and $G_{\alpha o}$ CA localization (Fig. 11). Almost no differences could be observed between endogenous and exogenous $G_{\alpha o}$ or $G_{\alpha o}$ CA subcellular distributions, but a more detailed observation showed that increasing the amounts of $G_{\alpha o}$ by $G_{\alpha o}$ or $G_{\alpha o}$ CA transfection lead to an increase in its signal in the cytoplasm area (cytoplasm plus Golgi). Further, this increase appeared to be even slightly higher for exogenous $G_{\alpha o}$ CA than for exogenous $G_{\alpha o}$. Nonetheless, this has to be further proved, by e.g. determining the PM-to-cytoplasm distribution ratio for each condition.

Next, we determined the subcellular colocalization sites for Wt, SA and SE APP-GFP with both $G_{\alpha o}$ and $G_{\alpha o}$ CA proteins. All the cotransfections were performed during the course of 6 h, since A) this was a time period when both proteins started to be expressed, and could be visually observed, and B) it was the only time point where $G_{\alpha o}$-induced STAT3 phosphorylation could be observed by WB means (see chapter 4.5.1). The images showed that APP-GFP proteins and transfected $G_{\alpha o}$ mainly colocalized at the PM, including in cellular projections, and at the Golgi and nearby cytoplasmic vesicles (Fig. 12). The quantitative analysis of the entire cell using Coloc2 plugin of Fiji showed that colocalization with $G_{\alpha o}$ was slightly higher for both SA and SE APP-GFPs when compared to Wt APP-GFP (Fig. 13). By analysing the cells

images, this difference in colocalization appeared to be more pronounced at the cellular projections. Quantitative colocalization analysis of these projections proved this to be true (statistically significant) only for the SA and not for the SE APP-GFP mutant (Fig. 13). A more careful examination of the cells images revealed that the $G_{\alpha o}$ localization is not itself altered, but that the APP S655 phosphomutants appear to localize, at a higher extent than the Wt APP-GFP, in subcellular sites where they can interact with $G_{\alpha o}$. For example, and as it was already reported, both APP-GFPs phosphomutants are more enriched in the PM (Vieira et al., 2009). Since $G_{\alpha o}$ is mainly localized in the PM, it is normal that both phosphomutants present higher colocalization with $G_{\alpha o}$. Further, both mutants spend also more time at the Golgi than the Wt APP-GFP (Vieira et al., 2009; Vieira et al., 2010), another structure where exogenous $G_{\alpha o}$ was also found enriched (Fig. 12).

Mimicking $G_{\alpha o}$ activation using the $G_{\alpha o}$ CA mutant resulted in only a slight increase in $G_{\alpha o}$/APP colocalization, and only for Wt (from 65% to 70%) and SE APP-GFPs (from 72% to 77%). Again, we could not observe an alteration in APP-GFP proteins subcellular localization with their cotransfection with constitutively active $G_{\alpha o}$ (Fig. 14). One hypothesis arises to explain this slightly higher colocalization: with activation, α subunits of heterotrimeric G proteins dissociate from the βγ subunit and from the respective GPCR so they are available to interact with their effector proteins, which may be localized inside the cell and not at the plasma membrane (Svoboda and Novotny, 2002; Hynes et al., 2004). This means increased $G_{\alpha o}$ CA distribution throughout the cell, increasing the probability of APP and $G_{\alpha o}$ to colocalize. This should be especially true for SE APP-GFP, since this mutant has an increased trafficking across the cell, in opposition to the SA mutant, which exits more difficultly from the PM and Golgi (Vieira et al., 2009).

Of note, all this colocalization data has to be interpreted with some caution, since exogenous $G_{\alpha o}$ appears to have a higher expression than APP-GFP, and since it is more widely distributed throughout the cell, the quantitative analysis yielded very high colocalization levels between both proteins, which probably does not all correspond to true colocalization. Besides projections, some cytoplasmic vesicles and the Golgi, it does not seem to exist true colocalization between $G_{\alpha o}$ and APP in the remaining subcellular locations. The same occurs with $G_{\alpha o}$ CA, which is highly expressed in cotransfected cells, causing the same problems with the colocalization analysis, yielding higher values than we would expect for true colocalization. Future work that could shed

more light on the effect of APP phosphorylation on $G_{\alpha o}$/APP colocalization will be to analyse the colocalization of APP-GFP proteins with the endogenous $G_{\alpha o}$. This way, $G_{\alpha o}$ expression should not be so high and thus colocalization analysis would be closer to the reality. Indeed, in order to better analyse potential sites of endogenous APP/$G_{\alpha o}$ colocalization, this was observed in non-transfected cells by ICC means. Results showed that endogenous APP and endogenous $G_{\alpha o}$ distributions are quite exclusive, with the PM being the main visible site of potential colocalization, while some colocalization appears to also occur nearby the Golgi (Fig. 16).

Interestingly, in these non-transfected cells labelled with anti-$G_{\alpha o}$ and 22C11, it was possible to observe that cells with more projections were expressing more $G_{\alpha o}$ (data not shown). Further, a previous study conducted in our lab showed that, upon 24h of transfection, APP-GFP not only slightly increased the number of processes in SH-SY5Y, but also increased their length, specially for the SE APP-GFP protein, with over 50% of transfected cells exhibiting pre-neurites (contrasting with less than 20% in N1 vector transfected cells) (Rocha, 2011). So, the next goal was to analyse if $G_{\alpha o}$/APP co-transfection induced morphological changes in SH-SY5Y cells, and if these were affected by S655 phosphorylation and $G_{\alpha o}$ activation.

First, non-transfected cells and pcDNA3 transfected cells were analysed to establish a control. As expected in undifferentiated SH-SY5Y cells, very few projections were visible (≈ 1 per cell), while transfection of the vector pcDNA3 alone increased this to ≈ 3 per cell (Fig. 17). When transfected with $G_{\alpha o}$, the number of projections increased significantly (doubled) relatively to vector-transfected cells, and most of the cells appeared highly plastic, with very small projections. This increased even more when $G_{\alpha o}$ was cotransfected with Wt APP-GFP but, unexpectedly, decreased when it was cotransfected with either the SA APP-GFP or SE APP-GFP proteins (Fig. 17), what was intriguing since their higher colocalization (Fig. 13). By its turn, $G_{\alpha o}$ activation alone, mimicked by the $G_{\alpha o}$ CA, also increased the number of projections over $G_{\alpha o}$ data (Fig. 18). However, the number of projections did not change for $G_{\alpha o}$ CA cotransfection with Wt or SE APP when compared to their $G_{\alpha o}$ respective transfections (Fig. 18). Since the number of projections in $G_{\alpha o}$ CA and $G_{\alpha o}$:Wt APP-GFP expressing cells is roughly the same, and Wt APP-GFP cotransfection with $G_{\alpha o}$ CA does not increase it, this indicates that APP cooperates with $G_{\alpha o}$ to increase the number of projections most probably via $G_{\alpha o}$ activation. Interestingly, $G_{\alpha o}$ CA:SA APP-GFP

cotransfection doubles the number of projections found in $G_{\alpha o}$:SA APP-GFP cells, but not above $G_{\alpha o}$ CA alone, indicating that SA is not able to activate $G_{\alpha o}$ or to alone direct it to a downstream pathway leading to the generation of projections. Nonetheless, SA APP-GFP does not hinder activated $G_{\alpha o}$ ($G_{\alpha o}$ CA) to follow that pathway, a phenomenon that actually occurs with the S655E APP-GFP mutant ($G_{\alpha o}$ and $G_{\alpha o}$ CA transfections had fewer projections). This mutant inhibits normal $G_{\alpha o}$ CA-induction of projections, potentially deviating it for other processes. Indeed, subsequent analysis confirmed that although both S655 phosphomutants did not increase the number of projections, they increased their length, as it could be seen in the microphotographs (Fig. 12 and 14) and by the increased number of cells with pre-neurites (Fig. 19 and 20). Interestingly, this finding correlates well with their higher colocalization with $G_{\alpha o}$ at the PM/cellular projections (Fig. 13 and 15). Noticeably, this elongation was longer for the $G_{\alpha o}$/SE co-transfection: more cells with pre-neurites and visually longer pre-neurites. Moreover, for $G_{\alpha o}$ CA, only when transfected alone or cotransfected with Wt APP-GFP we see a slight increase in the number of cells with pre-neurites when compared to $G_{\alpha o}$. This occurred with a much lower amplitude than the observed for the number of projections, indicating that activated $G_{\alpha o}$ is more prone to activate the formation of cellular projections rather than neuritic elongation. In opposition to Wt APP-GFP, $G_{\alpha o}$ CA cotransfection with the S655 phosphomutants does not change or even slightly decreases (S655A) neuritic elongation. All these suggest a hypothesis where, when at the PM (or specifically in projections), APP binds to and targets $G_{\alpha o}$ to a complex with other proteins that function in neuritic elongation. The binding strength of this cell surface APP/$G_{\alpha o}$ containing complex would be highly increased by APP S655 phosphorylation, which would 'sequestrate' active $G_{\alpha o}$ and target it to elongation. Dephospho S655 APP could also forms this complex at the PM but, if $G_{\alpha o}$ is already activated, APP would not be able to 'lock it' in the elongation complex/pathway, and part of activated $G_{\alpha o}$ (as it occurs with $G_{\alpha o}$ CA) would enter the alternative pathway of formation of projections.

In synthesis, these results show that, after short-term transfection, both proteins are important for neuritogenesis, either in for de novo formation of neurites or for neuritic elongation. Activated $G_{\alpha o}$ appears to be very important in the initial cytoskeleton modifications, such as the increase in the number of projections, with APP co-stimulating it, potentially by increasing $G_{\alpha o}$ activation. Colocalization at the PM and/or at cells projections is not the most important for co-stimulation of the number of

projections. By its turn, APP is very important for the elongation of the projections, with $G_{\alpha o}$ cooperating with APP potentially via the formation of a phospho S655 APP/$G_{\alpha o}$ complex with an unknown protein, such as GAP-43 and/or GRIN1. Another player of this mechanism can be sAPPα, a known neuritogenic factor, whose secretion is increased by S655 phosphorylation (Young-Pearse et al., 2008; Vieira et al., 2009). Of note, not only sAPPα but also membranar APP is necessary for neuritic elongation (Young-Pearse et al., 2008), and thus the higher cell surface locations for the S655 phosphomutants may underlie part of the mechanisms observed for their higher neuritic elongation. Remarkably, since SA normally does not elongate projections more than the Wt, this work places $G_{\alpha o}$ in this membranar APP/sAPP neuritogenic mechanism.

However, with these results it is still unclear if both proteins interact directly with each other or if they stimulate each other pathway at more downstream (or upstream) levels. The formation of APP/$G_{\alpha o}$ and APP/$G_{\alpha o}$/GRIN1 or GAP43 complexes and their colocalization at the PM will be very interesting to analyse.

Cytoskeleton proteins remodelling is an important step in the formation and stabilization of neurites (da Silva and Dotti, 2002). With that in mind, we analysed the expression of both tubulin and actin to see if $G_{\alpha o}$ or APP overexpression modified their levels. While there seems to exist a tendency to either $G_{\alpha o}$ or $G_{\alpha o}$ CA to decrease actin levels, and for all APP-GFP forms to increase it, what is more predominant is the high variability that exists between experiments (high standard error of the mean), with the same occurring for tubulin levels. Since actin and tubulin are normally very tightly controlled proteins, even with their β-isoforms being often used as loading controls, these great variations seem to indicate a high level of actin and microtubule remodelling occurring in the transfected cells, which agrees with the high number of projections induced by $G_{\alpha o}$ and/or APP expression, and/or their elongation. This remodelling is more pronounced when both proteins are cotransfected, corroborating with the findings that these proteins can cooperate in cytoskeleton remodelling.

Until this point we have already shown that APP and $G_{\alpha o}$ are responsible for several morphological changes resulting in neuritogenesis. Following, we went to test if these morphological changes could be related to $G_{\alpha o}$-induced STAT3 activation, but this was somewhat difficult, due to the existence of what appears to be a retro-inhibition mechanism. When cells were transfected for 6h with only $G_{\alpha o}$ or $G_{\alpha o}$ CA, a rise in

nuclear STAT3 levels was visible, indicating that indeed $G_{\alpha o}$ was capable of inducing STAT3 activation (Fig. 23 and 24). These results were also confirmed by WB assay (Fig. 25) although only for $G_{\alpha o}$, with no increases but rather decreases below control levels being observed for P-STAT3 upon $G_{\alpha o}$ CA transfection. Since $G_{\alpha o}$ CA is reported to increase P-STAT3 levels (Ram et al., 2000) this revealed that, following $G_{\alpha o}$/STAT3 activation, a retro-inhibition mechanism rapidly occurs. Indeed, this retro-inhibition is visible by ICC upon 24 h of transfection, where nSTAT3 levels had returned to levels equal or lower than in neighbour non-transfected cells. When phosphorylated, STAT3 dimerizes and is translocated to the nucleus, where it binds to DNA and acts as a transcriptional factor. However, this action is normally short-lived, with STAT3 being dephosphorylated only 15-30 min after entering the nucleus, which results in its export to the cytoplasm. For STAT3 signalling to be maintained, STAT3 must be continuous phosphorylated in the cytoplasm and shuttled to the nucleus (Pranada et al., 2004; Vinkemeier, 2004). In our experiment we are only seeing STAT3 accumulation in the nucleus upon 6 h of transfection, with the signalling almost disappearing at 24 h. This is not unique, since in most cases, STAT3 signalling is transient and involves retro-inhibition mechanisms (Schuringa, 2001). Some factors involved in this feedback have already been identified, such as the suppressors of cytokine signalling (SOCS) proteins, which are transcribed as a result of STAT3 activation, or by the action of protein phosphatases (Nicola and Greenhalgh, 2000; Tanuma et al., 2000). However, these proteins have only being described to interact with Jak/STAT signalling, so it is unclear if they are responsible for the retro-inhibition mechanism we are observing in our conditions.

When co-transfected with APP-GFP constructs, $G_{\alpha o}$ did not seem to activate STAT3, with all cotransfections mainly leading to lower or equal nSTAT3 intensities (qualitative analysis). Nonetheless, some activation was still visible, mainly for the Wt, correlating with its role in formation of projections, as it also increased when $G_{\alpha o}$ CA was cotransfected (Fig. 28). In contrast, $G_{\alpha o}$ cotransfection with SA and SE have lower induction of nSTAT3 levels (especially for SE), as depicted from qualitative and quantitative data. But while SA increases nSTAT3 intensity when cotransfected with $G_{\alpha o}$ CA, SE does not change or even decreases (Fig. 28 and 29). These results can either mean that A) APP is blocking $G_{\alpha o}$-induced STAT3 activation, or B) APP is accelerating $G_{\alpha o}$-induced STAT3 activation and consequent deactivation. We believe that the hypothesis B is the correct one, due to the morphological changes that are enhanced

when $G_{\alpha o}$ is cotransfected with APP and because, as seen by the qualitative analysis, there are still a few cells, even when APP SE is cotransfected, that exhibit high levels of nSTAT3. Another work being developed in our lab addressed this theme by analysing STAT3 Tyr705 phosphorylation in WB assays, and results showed a more pronounced $G_{\alpha o}$-induced STAT3 activation however, with cotransfection of APP constructs with either $G_{\alpha o}$ or $G_{\alpha o}$ CA, this activation decreased, consistent with the existence of a retro-inhibition effect (data not yet published). Also, recent studies indicate that sAPPα is able to induce STAT3 activation through the IL-6/gp130 signalling pathway, in alternative to the Src-Stat3 pathway activated by $G_{\alpha o}$ (Kwak et al., 2010). Since phosphorylation of S655 induces a higher production of sAPPα (Vieira et al., 2009), retro-inhibition following a faster/greater STAT3 activation would explain why cells co-transfected with SE APP-GFP and $G_{\alpha o}$ CA showed the lowest number of high nSTAT3 and the highest of lower nSTAT3.

Interestingly, the profiles of nSTAT3 intensities with APP-GFP and $G_{\alpha o}$ co-transfections (Fig. 28 and 29) correlate well with the profiles of number of projections (Fig. 17 and 18). Further, the cotransfection with longer neurites (SE/$G_{\alpha o}$) leads to the highest nSTAT3 retro-inhibition, suggesting a correlation between neuritic elongation and a pre-activated and already retro-inhibited STAT3 signalling. Also, besides STAT3, there is a possibility that both $G_{\alpha o}$ and APP are activating other neuritogenic pathways. As been already mentioned, $G_{\alpha o}$ has also been shown to induce neuritogenesis through interaction with GRIN1, which leads to activation of cdc42, a member of the Rho family of GTPases (Nakata and Kozasa, 2005). Moreover, sAPPα has been described as an inducer of neuritogenesis through the activation of the mitogen-activated protein kinase (MAPK) pathway (Gakhar-Koppole et al., 2008).

6. Conclusion

This work provided evidences that $G_{\alpha o}$ and APP are important for inducing morphological alterations related to neuritogenesis, with $G_{\alpha o}$ having an essential role in inducing the initial formation of cellular projections, probably by activating the STAT3 pathway, and APP being important for their elongation. APP was observed to highly cooperate with $G_{\alpha o}$ in the formation of cellular projections, most probably via $G_{\alpha o}$ activation, while $G_{\alpha o}$ appears to be a part of an alternative APP-dependent neuritic elongation mechanism, enhanced by APP S655 phosphorylation. However, their interactive play in these mechanisms still need further clarification, including the role played by APP and its phosphorylation in $G_{\alpha o}$-induced neuritogenesis and STAT3 activation. Further work will comprehend e.g. the morphological evaluation of a higher number of cells to certify these findings, the analysis of STAT3 activation by ICC using APP-GFP, a mouse anti-$G_{\alpha o}$ antibody and the rabbit anti-P-STAT3 antibody, and the analysis of relevant APP/$G_{\alpha o}$ complexes and other neuritogenic pathways that may be being influenced by APP and $G_{\alpha o}$ activity. These results prove that these proteins functionally interact, and their potential value in neuritogenic therapeutic applications will be further studied.

References

Ahnert-Hilger, G., Nurnberg, B., Exner, T., Schafer, T. and Jahn, R. (1998). "**The heterotrimeric G protein Go2 regulates catecholamine uptake by secretory vesicles.**" EMBO J 17(2): 406-413.

Ahnert-Hilger, G., Schafer, T., Spicher, K., Grund, C., Schultz, G. and Wiedenmann, B. (1994). "**Detection of G-protein heterotrimers on large dense core and small synaptic vesicles of neuroendocrine and neuronal cells.**" Eur J Cell Biol 65(1): 26-38.

Allinquant, B., Hantraye, P., Mailleux, P., Moya, K., Bouillot, C. and Prochiantz, A. (1995). "**Downregulation of amyloid precursor protein inhibits neurite outgrowth in vitro.**" J Cell Biol 128(5): 919-927.

Antonelli, V., Bernasconi, F., Wong, Y. H. and Vallar, L. (2000). "**Activation of B-Raf and regulation of the mitogen-activated protein kinase pathway by the G(o) alpha chain.**" Mol Biol Cell 11(4): 1129-1142.

Brabet, P., Dumuis, A., Sebben, M., Pantaloni, C., Bockaert, J. and Homburger, V. (1988). "**Immunocytochemical localization of the guanine nucleotide-binding protein Go in primary cultures of neuronal and glial cells.**" J Neurosci 8(2): 701-708.

Brabet, P., Pantaloni, C., Bockaert, J. and Homburger, V. (1991). "**Metabolism of two Go alpha isoforms in neuronal cells during differentiation.**" J Biol Chem 266(20): 12825-12828.

Brouillet, E., Trembleau, A., Galanaud, D., Volovitch, M., Bouillot, C., Valenza, C., Prochiantz, A. and Allinquant, B. (1999). "**The amyloid precursor protein interacts with Go heterotrimeric protein within a cell compartment specialized in signal transduction.**" J Neurosci 19(5): 1717-1727.

Caulfield, M. P., Jones, S., Vallis, Y., Buckley, N. J., Kim, G. D., Milligan, G. and Brown, D. A. (1994). "**Muscarinic M-current inhibition via G alpha q/11 and alpha-adrenoceptor inhibition of Ca2+ current via G alpha o in rat sympathetic neurones.**" J Physiol 477 (Pt 3): 415-422.

Chow, V. W., Mattson, M. P., Wong, P. C. and Gleichmann, M. (2010). "**An overview of APP processing enzymes and products.**" Neuromolecular Med 12(1): 1-12.

Cismowski, M. J., Ma, C. L., Ribas, C., Xie, X. B., Spruyt, M., Lizano, J. S., Lanier, S. M. and Duzic, E. (2000). "**Activation of heterotrimeric G-protein signaling by a**

Ras-related protein - Implications for signal integration." Journal of Biological Chemistry 275(31): 23421-23424.

Cole, S. L. and Vassar, R. (2008). "**The role of amyloid precursor protein processing by BACE1, the beta-secretase, in Alzheimer disease pathophysiology.**" J Biol Chem 283(44): 29621-29625.

da Cruz e Silva, E. F. and da Cruz e Silva, O. A. (2003). "**Protein phosphorylation and APP metabolism.**" Neurochem Res 28(10): 1553-1561.

da Silva, J. S. and Dotti, C. G. (2002). "**Breaking the neuronal sphere: regulation of the actin cytoskeleton in neuritogenesis.**" Nat Rev Neurosci 3(9): 694-704.

De Vries, L., Zheng, B., Fischer, T., Elenko, E. and Farquhar, M. G. (2000). "**The regulator of G protein signaling family.**" Annu Rev Pharmacol Toxicol 40: 235-271.

Diverse-Pierluissi, M. A., Fischer, T., Jordan, J. D., Schiff, M., Ortiz, D. F., Farquhar, M. G. and De Vries, L. (1999). "**Regulators of G protein signaling proteins as determinants of the rate of desensitization of presynaptic calcium channels.**" J Biol Chem 274(20): 14490-14494.

Gabrion, J., Brabet, P., Nguyen Than Dao, B., Homburger, V., Dumuis, A., Sebben, M., Rouot, B. and Bockaert, J. (1989). "**Ultrastructural localization of the GTP-binding protein Go in neurons.**" Cell Signal 1(1): 107-123.

Gakhar-Koppole, N., Hundeshagen, P., Mandl, C., Weyer, S. W., Allinquant, B., Muller, U. and Ciccolini, F. (2008). "**Activity requires soluble amyloid precursor protein alpha to promote neurite outgrowth in neural stem cell-derived neurons via activation of the MAPK pathway.**" Eur J Neurosci 28(5): 871-882.

Giambarella, U., Yamatsuji, T., Okamoto, T., Matsui, T., Ikezu, T., Murayama, Y., Levine, M. A., Katz, A., Gautam, N. and Nishimoto, I. (1997). "**G protein betagamma complex-mediated apoptosis by familial Alzheimer's disease mutant of APP.**" EMBO J 16(16): 4897-4907.

Gomperts, B. D., Tatham, P. E. R. and Kramer, I. M. (2009). Signal transduction. Academic Press, 2nd edition.

Hankey, P. A. (2009). "**Regulation of hematopoietic cell development and function by Stat3.**" Front Biosci 14: 5273-5290.

Hardy, J. (1992). "**Framing beta-amyloid.**" Nat Genet 1(4): 233-234.

Hardy, J. A. and Higgins, G. A. (1992). "**Alzheimer's disease: the amyloid cascade hypothesis.**" Science 256(5054): 184-185.

He, J. C., Gomes, I., Nguyen, T., Jayaram, G., Ram, P. T., Devi, L. A. and Iyengar, R. (2005). "**The G alpha(o/i)-coupled cannabinoid receptor-mediated neurite outgrowth involves Rap regulation of Src and Stat3.**" J Biol Chem 280(39): 33426-33434.

Henriques, A. G., Vieira, S. I., da Cruz, E. S. E. F. and da Cruz, E. S. O. A. (2010). "**Abeta promotes Alzheimer's disease-like cytoskeleton abnormalities with consequences to APP processing in neurons.**" J Neurochem 113(3): 761-771.

Hille, B. (1994). "**Modulation of ion-channel function by G-protein-coupled receptors.**" Trends Neurosci 17(12): 531-536.

Holz, G. G. t., Rane, S. G. and Dunlap, K. (1986). "**GTP-binding proteins mediate transmitter inhibition of voltage-dependent calcium channels.**" Nature 319(6055): 670-672.

Hsu, W. H., Rudolph, U., Sanford, J., Bertrand, P., Olate, J., Nelson, C., Moss, L. G., Boyd, A. E., Codina, J. and Birnbaumer, L. (1990). "**Molecular cloning of a novel splice variant of the alpha subunit of the mammalian Go protein.**" J Biol Chem 265(19): 11220-11226.

Huang, C. L., Jan, Y. N. and Jan, L. Y. (1997). "**Binding of the G protein betagamma subunit to multiple regions of G protein-gated inward-rectifying K+ channels.**" FEBS Lett 405(3): 291-298.

Hynes, T. R., Hughes, T. E. and Berlot, C. H. (2004). "**Cellular localization of GFP-tagged alpha subunits.**" Methods Mol Biol 237: 233-246.

Jiang, M. and Bajpayee, N. S. (2009). "**Molecular mechanisms of go signaling.**" Neurosignals 17(1): 23-41.

Jiang, M., Gold, M. S., Boulay, G., Spicher, K., Peyton, M., Brabet, P., Srinivasan, Y., Rudolph, U., Ellison, G. and Birnbaumer, L. (1998). "**Multiple neurological abnormalities in mice deficient in the G protein Go.**" Proc Natl Acad Sci U S A 95(6): 3269-3274.

Karlinsky, H., Vaula, G., Haines, J. L., Ridgley, J., Bergeron, C., Mortilla, M., Tupler, R. G., Percy, M. E., Robitaille, Y., Noldy, N. E. and et al. (1992). "**Molecular and prospective phenotypic characterization of a pedigree with familial Alzheimer's**

disease and a missense mutation in codon 717 of the beta-amyloid precursor protein gene." Neurology 42(8): 1445-1453.

Kroeze, W. K., Sheffler, D. J. and Roth, B. L. (2003). "**G-protein-coupled receptors at a glance.**" J Cell Sci 116(Pt 24): 4867-4869.

Kwak, Y. D., Dantuma, E., Merchant, S., Bushnev, S. and Sugaya, K. (2010). "**Amyloid-beta precursor protein induces glial differentiation of neural progenitor cells by activation of the IL-6/gp130 signaling pathway.**" Neurotox Res 18(3-4): 328-338.

Landmann, L. and Marbet, P. (2004). "**Colocalization analysis yields superior results after image restoration.**" Microsc Res Tech 64(2): 103-112.

Lang, J. (1989). "**Purification and characterization of subforms of the guanine-nucleotide-binding proteins G alpha i and G alpha o.**" Eur J Biochem 183(3): 687-692.

Lehninger, A. L., Nelson, D. L. and Cox, M. M. (2005). Lehninger principles of biochemistry. W.H. Freeman, 4th edition.

Lei, Q., Jones, M. B., Talley, E. M., Schrier, A. D., McIntire, W. E., Garrison, J. C. and Bayliss, D. A. (2000). "**Activation and inhibition of G protein-coupled inwardly rectifying potassium (Kir3) channels by G protein beta gamma subunits.**" Proc Natl Acad Sci U S A 97(17): 9771-9776.

Ling, Y., Morgan, K. and Kalsheker, N. (2003). "**Amyloid precursor protein (APP) and the biology of proteolytic processing: relevance to Alzheimer's disease.**" Int J Biochem Cell Biol 35(11): 1505-1535.

Locht, C., Coutte, L. and Mielcarek, N. (2011). "**The ins and outs of pertussis toxin.**" FEBS J 278(23): 4668-4682.

Lodish, H. F. (2003). Molecular cell biology. W.H. Freeman and Company, 5th edition.

Manders, E. M. M., Verbeek, F. J. and Aten, J. A. (1993). "**Measurement of co-localization of objects in dual-colour confocal images.**" Journal of Microscopy 169(3): 375-382.

Milligan, G. and Kostenis, E. (2006). "**Heterotrimeric G-proteins: a short history.**" Br J Pharmacol 147 Suppl 1: S46-55.

Milward, E. A., Papadopoulos, R., Fuller, S. J., Moir, R. D., Small, D., Beyreuther, K. and Masters, C. L. (1992). "**The amyloid protein precursor of Alzheimer's disease is a mediator of the effects of nerve growth factor on neurite outgrowth.**" Neuron 9(1): 129-137.

Mullaney, I. and Milligan, G. (1989). "**Elevated levels of the guanine nucleotide binding protein, Go, are associated with differentiation of neuroblastoma x glioma hybrid cells.**" FEBS Lett 244(1): 113-118.

Murtagh, J. J., Jr., Eddy, R., Shows, T. B., Moss, J. and Vaughan, M. (1991). "**Different forms of Go alpha mRNA arise by alternative splicing of transcripts from a single gene on human chromosome 16.**" Mol Cell Biol 11(2): 1146-1155.

Nakata, H. and Kozasa, T. (2005). "**Functional characterization of Galphao signaling through G protein-regulated inducer of neurite outgrowth 1.**" Mol Pharmacol 67(3): 695-702.

Nicola, N. A. and Greenhalgh, C. J. (2000). "**The suppressors of cytokine signaling (SOCS) proteins: important feedback inhibitors of cytokine action.**" Exp Hematol 28(10): 1105-1112.

Nishimoto, I., Okamoto, T., Matsuura, Y., Takahashi, S., Murayama, Y. and Ogata, E. (1993). "**Alzheimer amyloid protein precursor complexes with brain GTP-binding protein G(o).**" Nature 362(6415): 75-79.

Offermanns, S. (2003). "**G-proteins as transducers in transmembrane signalling.**" Prog Biophys Mol Biol 83(2): 101-130.

Okamoto, T., Takeda, S., Giambarella, U., Murayama, Y., Matsui, T., Katada, T., Matsuura, Y. and Nishimoto, I. (1996). "**Intrinsic signaling function of APP as a novel target of three V642 mutations linked to familial Alzheimer's disease.**" EMBO J 15(15): 3769-3777.

Okamoto, T., Takeda, S., Murayama, Y., Ogata, E. and Nishimoto, I. (1995). "**Ligand-dependent G protein coupling function of amyloid transmembrane precursor.**" J Biol Chem 270(9): 4205-4208.

Pranada, A. L., Metz, S., Herrmann, A., Heinrich, P. C. and Muller-Newen, G. (2004). "**Real time analysis of STAT3 nucleocytoplasmic shuttling.**" J Biol Chem 279(15): 15114-15123.

Ram, P. T., Horvath, C. M. and Iyengar, R. (2000). "**Stat3-mediated transformation of NIH-3T3 cells by the constitutively active Q205L Galphao protein.**" Science 287(5450): 142-144.

Riobo, N. A. and Manning, D. R. (2005). "**Receptors coupled to heterotrimeric G proteins of the G12 family.**" Trends Pharmacol Sci 26(3): 146-154.

Rocha, J. F. d. 2011. "**Understanding APP-dependent neuronal differentiation.**" Master, Health Sciences Department, University of Aveiro

Roman, D. L. and Traynor, J. R. (2011). "**Regulators of G protein signaling (RGS) proteins as drug targets: modulating G-protein-coupled receptor (GPCR) signal transduction.**" J Med Chem 54(21): 7433-7440.

Romero-Calvo, I., Ocon, B., Martinez-Moya, P., Suarez, M. D., Zarzuelo, A., Martinez-Augustin, O. and de Medina, F. S. (2010). "**Reversible Ponceau staining as a loading control alternative to actin in Western blots.**" Anal Biochem 401(2): 318-320.

Scherer, F., Anton, M., Schillinger, U., Henke, J., Bergemann, C., Kruger, A., Gansbacher, B. and Plank, C. (2002). "**Magnetofection: enhancing and targeting gene delivery by magnetic force in vitro and in vivo.**" Gene Ther 9(2): 102-109.

Schettini, G., Govoni, S., Racchi, M. and Rodriguez, G. (2010). "**Phosphorylation of APP-CTF-AICD domains and interaction with adaptor proteins: signal transduction and/or transcriptional role--relevance for Alzheimer pathology.**" J Neurochem 115(6): 1299-1308.

Schuringa, J.-J. 2001. "**Molecular analyses and biological implications of STAT3 signal transduction.**" Faculty of Mathematics and Natural Sciences, University of Groningen

Sehgal, P. B. (2008). "**Paradigm shifts in the cell biology of STAT signaling.**" Semin Cell Dev Biol 19(4): 329-340.

Siderovski, D. P., Diverse-Pierluissi, M. and De Vries, L. (1999). "**The GoLoco motif: a Galphai/o binding motif and potential guanine-nucleotide exchange factor.**" Trends Biochem Sci 24(9): 340-341.

Siderovski, D. P. and Willard, F. S. (2005). "**The GAPs, GEFs, and GDIs of heterotrimeric G-protein alpha subunits.**" Int J Biol Sci 1(2): 51-66.

Simonds, W. F. (1999). "**G protein regulation of adenylate cyclase.**" Trends Pharmacol Sci 20(2): 66-73.

Small, D. H. (1998). "**The role of the amyloid protein precursor (APP) in Alzheimer's disease: does the normal function of APP explain the topography of neurodegeneration?**" Neurochem Res 23(5): 795-806.

Small, S. A. and Gandy, S. (2006). "**Sorting through the cell biology of Alzheimer's disease: intracellular pathways to pathogenesis.**" Neuron 52(1): 15-31.

Smine, A., Xu, X., Nishiyama, K., Katada, T., Gambetti, P., Yadav, S. P., Wu, X., Shi, Y. C., Yasuhara, S., Homburger, V. and Okamoto, T. (1998). "**Regulation of brain G-protein go by Alzheimer's disease gene presenilin-1.**" J Biol Chem 273(26): 16281-16288.

Sommer, B. (2002). "**Alzheimer's disease and the amyloid cascade hypothesis: ten years on.**" Curr Opin Pharmacol 2(1): 87-92.

Sternweis, P. C. and Robishaw, J. D. (1984). "**Isolation of two proteins with high affinity for guanine nucleotides from membranes of bovine brain.**" J Biol Chem 259(22): 13806-13813.

Strittmatter, S. M., Igarashi, M. and Fishman, M. C. (1994). "**GAP-43 amino terminal peptides modulate growth cone morphology and neurite outgrowth.**" J Neurosci 14(9): 5503-5513.

Strittmatter, S. M., Valenzuela, D., Sudo, Y., Linder, M. E. and Fishman, M. C. (1991). "**An intracellular guanine nucleotide release protein for G0. GAP-43 stimulates isolated alpha subunits by a novel mechanism.**" J Biol Chem 266(33): 22465-22471.

Suzuki, T. and Nakaya, T. (2008). "**Regulation of amyloid beta-protein precursor by phosphorylation and protein interactions.**" J Biol Chem 283(44): 29633-29637.

Svoboda, P. and Novotny, J. (2002). "**Hormone-induced subcellular redistribution of trimeric G proteins.**" Cell Mol Life Sci 59(3): 501-512.

Tanuma, N., Nakamura, K., Shima, H. and Kikuchi, K. (2000). "**Protein-tyrosine phosphatase PTPepsilon C inhibits Jak-STAT signaling and differentiation induced by interleukin-6 and leukemia inhibitory factor in M1 leukemia cells.**" J Biol Chem 275(36): 28216-28221.

Thinakaran, G. and Koo, E. H. (2008). "**Amyloid precursor protein trafficking, processing, and function.**" J Biol Chem 283(44): 29615-29619.

Tsukamoto, T., Toyama, R., Itoh, H., Kozasa, T., Matsuoka, M. and Kaziro, Y. (1991). "**Structure of the human gene and two rat cDNAs encoding the alpha chain of GTP-binding regulatory protein Go: two different mRNAs are generated by alternative splicing.**" Proc Natl Acad Sci U S A 88(8): 2974-2978.

VanDongen, A. M., Codina, J., Olate, J., Mattera, R., Joho, R., Birnbaumer, L. and Brown, A. M. (1988). "**Newly identified brain potassium channels gated by the guanine nucleotide binding protein Go.**" Science 242(4884): 1433-1437.

Vieira, S. I., Rebelo, S., Domingues, S. C., da Cruz e Silva, E. F. and da Cruz e Silva, O. A. (2009). "**S655 phosphorylation enhances APP secretory traffic.**" Mol Cell Biochem 328(1-2): 145-154.

Vieira, S. I., Rebelo, S., Esselmann, H., Wiltfang, J., Lah, J., Lane, R., Small, S. A., Gandy, S., da Cruz, E. S. E. F. and da Cruz, E. S. O. A. (2010). "**Retrieval of the Alzheimer's amyloid precursor protein from the endosome to the TGN is S655 phosphorylation state-dependent and retromer-mediated.**" Mol Neurodegener 5: 40.

Vinkemeier, U. (2004). "**Getting the message across, STAT! Design principles of a molecular signaling circuit.**" J Cell Biol 167(2): 197-201.

Walter, J., Capell, A., Hung, A. Y., Langen, H., Schnolzer, M., Thinakaran, G., Sisodia, S. S., Selkoe, D. J. and Haass, C. (1997). "**Ectodomain phosphorylation of beta-amyloid precursor protein at two distinct cellular locations.**" J Biol Chem 272(3): 1896-1903.

Wolf, W. P., Spicher, K., Haase, H. and Schulze, W. (1998). "**Immunocytochemical localization of the G-protein sub-unit, G(o) alpha, in rat heart. Implications for a role of G(o) alpha in secretion of cardiac hormones.**" J Mol Cell Cardiol 30(6): 1149-1162.

Worley, P. F., Baraban, J. M., Van Dop, C., Neer, E. J. and Snyder, S. H. (1986). "**Go, a guanine nucleotide-binding protein: immunohistochemical localization in rat brain resembles distribution of second messenger systems.**" Proc Natl Acad Sci U S A 83(12): 4561-4565.

Xie, R., Li, L., Goshima, Y. and Strittmatter, S. M. (1995). "**An activated mutant of the alpha subunit of G(o) increases neurite outgrowth via protein kinase C.**" Brain Res Dev Brain Res 87(1): 77-86.

Yamatsuji, T., Okamoto, T., Takeda, S., Murayama, Y., Tanaka, N. and Nishimoto, I. (1996). "**Expression of V642 APP mutant causes cellular apoptosis as Alzheimer trait-linked phenotype.**" EMBO J 15(3): 498-509.

Young-Pearse, T. L., Chen, A. C., Chang, R., Marquez, C. and Selkoe, D. J. (2008). "**Secreted APP regulates the function of full-length APP in neurite outgrowth through interaction with integrin beta1.**" Neural Dev 3: 15.

Zheng, H. and Koo, E. H. (2011). "**Biology and pathophysiology of the amyloid precursor protein.**" Mol Neurodegener 6(1): 27.

Appendix

cDNA amplification and purification solutions

Luria-Bertani (LB) growth medium with Ampicillin:

For a final volume of 1 L, dissolve 25 g of LB (Merck) in deionised water. Adjust the volume up to 1 L of deionised water and autoclave the solution (the LB will mix during autoclaving). Let the medium cool down to 60ºC and add 1 mL of ampicillin of a 50 mg/mL stock solution.

Super Optimal broth with Catabolite repression (SOC) medium:

For a final volume of 1 L, dissolve 25,5g of SOB broth (Sigma-Aldrich) in deionised water. Shake until the solute is dissolved, add 10 mL of 250 mM KCL solution, adjust the pH to 7.0 with 5 N of sodium hydroxide and adjust the final volume up to 1 L with deionised water. Sterilize by autoclaving, cool it down to about 60ºC and add 20 mL of a sterile 1M glucose solution.

Cell Resuspension Solution:

- 50 mM of Tris-HCl (pH 7,5)
- 10 mM of EDTA
- 100 μg/mL of RNase A

Cell Lysis Solution:

- 0.2 M of sodium hydroxide
- 1% of SDS

Neutralization Solution:

- 1.32 M of potassium acetate (pH 4.8)

Neutralization Solution:

- 80 mM of potassium acetate
- 8.3 mM of Tris-HCl (pH 7.5)

- 40 μM of EDTA
- 55% of ethanol

Cell Culture and Immunocytochemistry Solutions

PBS (1x):

For a final volume of 500 mL, dissolve one pack of BupH Modified Dulbecco's Phosphate Buffered Saline Pack (Pierce) in deionised water. Final composition:

- 8 mM Sodium Phosphate
- 2 mM Potassium Phosphate
- 140 mM Sodium Chloride
- 10 mM Potassim Chloride

Sterilize by filtering the solution through a 0,2 μm filter and store it at 4ºC.

10% FBS MEM:F12 (1:1):

For a final volume of 1 L dissolve the next substances in deionised water:

- 4,805 g of MEM (Gibco, Invitrogen)
- 5,315 g of F12 (Gibco, Invitrogen)
- 1,5 g of NaHCO3 (Sigma)
- 0,055 g of Sodium pyruvate (Sigma)
- 10 mL of Streptomycin/Penicillin/Amphotericin solution (Gibco, Invitrogen)
- 100 mL of 10% FBS (Gibco, Invitrogen)
- 2,5 mL of L-glutamine (200 mM stock solution)

Adjust the pH to 7,3 and then adjust the volume to 1 L with deionised water.

4% Paraformaldehyde:

For a final volume of 100 mL, dissolve 4 g of paraformaldehyde in 100 mL of PBS 1X. Boil the solution at 58ºC, add a few drops of 1M sodium hydroxide for a better dissolution of the paraformaldehyde (only if necessary) and filter the final solution. Store at RT, away from light sources.

SDS-PAGE and Western Blot solutions

Lower Gel Buffer (LGB) 4x:

To a final volume of 1 L, add to deionised water the following:

- 181,65 g of Tris (1,5 M)
- 4 g of SDS (0,4%)

Mix to solve the solutes, adjust the pH to 8.9 and the volume to 1 L with deionised water. Store at 4ºC.

Upper Gel Buffer (UGB) 5x:

To a final volume of 1 L, add to deionised water:

- 75,69 g of Tris (0,5 M)

Mix to solve the solutes, adjust the pH to 6.8 and the volume to 1 L with deionised water. Store at 4ºC.

30% Acrylamide/0,8% Bisacrylamide:

To a final volume of 100 mL, add to deionised water the following:

- 29,2 g of Acrylamide
-0,8 g of Bisacrylamide

Mix to solve the solutes, adjust the volume to 100 mL with deionised water and filter trhough a 0,2 μm filter. Store at 4ºC.

10% ammonium persulfate (APS):

Right before use, dissolve 1 g of APS in 10 mL of deionised water.

10% sodium dodecylsulfate (SDS):

Dissolve 1 g of SDS in 10 ml of deionised water.

1 M Tris solution (pH 6.8):

To a final volume of 250 mL, add to deionised water:

- 30,3 g of Tris base

Adjust the pH to 6.8 and the volume to 250 mL.

Loading Gel Buffer (4x):

Mix the following reagents:

- 2,5 mL of 1M Tris solution (pH 6.8) (250 mM)
- 0,8 g of SDS (8%)
- 4 mL of glycerol (40%)
- 2 mL of β-mercaptoethanol (2%)
- 1 mg of Bromophenol blue (0,01%)

Adjust the volume to 10 mL with deionised water. Store at room temperature, away from light sources.

Running Buffer (10x):

To a final volume of 1 L, add to deionised water the following:

- 30,3 g of Tris (250 mM)
- 144,2 g of Glycine (2,5 M)
- 10 g of SDS (1%)

Mix to dissolve, adjust the pH to 8.3 and the volume to 1 L with deionised water.

Resolving (lower) gel solution:

For a final volume of 60 mL mix the following reagents:

	10 % gel	and	**20%** gel
- Deionised water	17,4 mL		2,2 mL
- 30% Acryl/0,8% Bisacryl solution	5 mL		20 mL
- LGB (4x)	7,5 mL		7,5mL
- 10% APS	150 µL		150 µL
- TEMED	15 µL		15 µL

Stacking (upper) gel solution:

For a 3,5 % gel with a final volume of 60 mL mix the following reagents:

- 13,2 mL of deionised water
- 2,4 ml of 30% Acryl/0,8% Bisacryl solution
- 4 mL of UGB (5x)
- 200 μL of 10% SDS
- 200 μL of 10% APS
- 20 μL of TEMED

Transfer Buffer (1x):

For a final volume of 1 L dissolve the following solutes in deionised water:

- 3,03 g of Tris (25 mM)
- 14,41 g of Glycine (192 mM)

Mix until dissolution is complete and adjust the pH to 8.3. Adjust the volume to 800 mL with deionised water, and just prior to use add 200 mL of methanol.

Tris buffered saline (TBS) 10x:

For a final volume of 1 L dissolve the following solutes in deionised water:

- 12,11 g of Tris (10 mM)
- 87,66 g of NaCl (150 mM)

Adjust the pH to 8.0, and the volume to 1 L with deionised water.

TBS plus Tween (TBS-T) 10x:

For a final volume of 1 L dissolve the following solutes in deionised water:

- 12,11 g of Tris (10 mM)
- 87,66 g of NaCl (150 mM)

- 5 mL of Tween 20 (0,05%)

Adjust the pH to 8.0, and the volume to 1 L with deionised water.